msc- 14964

14690-H003-R0-00
JANUARY 1972
NASA CONTRACT 9-10435

THERMAL NETWORK MODELING HANDBOOK

TRW SYSTEMS

Prepared for:
National Aeronautics and Space Administration
Manned Spacecraft Center
Under Contract NAS 9-10435

Prepared by:

Environmental and Thermal Systems Section
Applied Mechanics Department

Concurrence:

Robert R. McMurchy
Environmental and Thermal Systems Section

Concurrence:

Robert G. Payne, Manager
Applied Mechanics Department

Concurrence:

Robert L. Dotts
NASA Technical Monitor
NASA Manned Spacecraft Center

FOREWORD

This thermal network modelling handbook was generated under Task No. 4 of NASA Contract NAS 9-10435 entitled "Advanced SINDA Thermal Analyzer Development."

Under the total contract, three tasks were devoted to documentation: Task No. 1 for development of the User's Manual, TRW Report No. 14690-H001-R0-00, April 1971, Task No. 2 for development of the Program Manual, TRW Report No. 14690-H002-R0-00, June 1971, and Task No. 4 for development of the Thermal Network Modelling Handbook contained herein.

Contrasted to the User's Manual and Program Manual which describe the complete usage and content of the SINDA Computer Program, a complete manuscript describing all the complexities of Thermal Mathematical Modelling was far beyond the scope and budgetary allocations of this task. Hence, this document was intended to serve as an initial building block for a future comprehensive document. Using this guideline a three-fold purpose was established: (1) to acquaint the new user with the terminology and concepts used in thermal mathematical modelling, (2) to present the more experienced and occasional user with quick formulae and methods for solving everyday problems, coupled with study cases which lend insight into the relationships that exist among the various solution techniques and parameters, and (3) to begin to catalogue in an orderly fashion the common formulae which in the future may be applied to automated conversational language techniques.

TABLE OF CONTENTS

LIST OF FIGURES

LIST OF TABLES

NOMENCLATURE

A	=	Area
C	=	Thermal Capacitance
C_p	=	Specific heat
D	=	Diameter
D_H	=	Hydraulic diameter
E	=	Voltage
F	=	Radiation configuration (form) factor
G	=	Thermal conductance
h	=	Convective heat transfer coefficient
L	=	Length or running length
I	=	Current
k	=	Thermal conductivity
$\dot{m}$	=	Mass flow rate
n	=	Arbitrary exponent
N	=	Number of iterations
$\dot{Q}$	=	Heat rate
r	=	Radius
R	=	Resistance
t	=	Time
T	=	Temperature
T_∞	=	Surrounding media or free stream temperature
U	=	Velocity
U_∞	=	Free stream velocity
V	=	Volume
$\dot{W}$	=	Flow rate
w_s	=	Sampling frequency
w_c	=	Maximum frequency component
x	=	Arbitrary distance

NOMENCLATURE (Concluded)

ΔT = Temperature difference

$\mathcal{F}$ = Script-F (grey body from factor)

α = Thermal diffusivity

β = Coefficient of volumetric expansion

ρ = Density

σ = Stephan-Boltzmann constant

τ = Stability factor

ϵ = Emittance

Θ = Angle

λ = Radiation linearization factor

δ = Convergence criterion (relaxation criterion)

ζ = Damping factor

Symbols, subscripts and units not specifically mentioned in the Nomenclature are explained at the point of usage within the text.

1.0 INTRODUCTION

1.1 Thermal Math Modeling as a Cognitive Process

A brief introduction to the rudimentary techniques of thermal modeling coupled with a simple understanding of the various basic heat transfer mechanisms are the prerequisites for a beginning thermal math modeler. Properly applied, the body of concepts, principles and techniques applicable to thermal math modeling constitutes a valid engineering tool which can be applied to the solution of real engineering problems. A good lumped parameter representation of a thermal system requires, in addition to the basic principles and techniques, an elusive mixture of experience (with real systems, both physical and model) and Engineering Judgement to transfer the end product into an accurate, versatile and cost effective thermal math model.

Generally, the problems encountered in developing a thermal math model reduce to an overall object of achieving the greatest accuracy for the least cost. Cost factors are rather well defined, and fall into two classes: (1) the cost of developing the model, and (2) the cost of using the model. Development costs can be based almost solely on the actual engineering manpower required to do the job within the constraints of time and budget. However, the potential costs involved in using a model are often not as obvious nor as linear. For example, most thermal math models will be analyzed on a computer which is highly prioritized. In such an environment, a relatively small increase in required processor time, perhaps from 5 minutes to 15 minutes, often results in a reduced job priority and a corresponding slowdown in turnaround time, perhaps from one day to one week.

The problem of achieving accuracy in a math model, while subject to cost constraints, varies greatly from one thermal math model to another. General accuracy requirements may be as straight forward as "temperature accuracy shall be compatible with thermocouple A/D converter quantization error," or "... thermostat hysteresis." On the other hand, accuracy levels

might be indirectly indicated by requiring that a model must "be sufficiently detailed to permit meaningful parametric analyses with respect to insulation thickness variations in increments of 1/4 inch." Clearly, there is going to be a great deal of Engineering Judgement involved in developing a model that is "sufficiently detailed" to be "meaningful."

Succeeding sections of this report will present many of the basic principles and techniques involved in thermal math modeling. Experience, of course, can only be acquired from hands-on familiarity with real thermal systems and participation in the modeling and analysis thereof. Engineering Judgement can probably be described more accurately as the result of abstracting from the body of unique familiar information, a general understanding which can be extended to guide the investigation and comprehension of new and unfamiliar areas. As such, Engineering Judgement cannot be presented in a table, or a figure, or even an entire book. However, it is possible to present a collection and discussion of examples of thermal math modeling which will serve, not as a source of practical experience, but as a body of unique and familiar information from which the reader may abstract as much Engineering Judgement as he is able. Such a collection is included in the latter half of this report.

2.0 THERMAL MATHEMATICAL MODELING

2.1 Network Solution

Two systems are said to be analogous when they both have similar equations and boundary conditions; and the equations describing the behavior of one system can be transformed into the equations for the other by simply changing symbols of the variables. Thermal and electrical systems are two such analogous systems as shown in table 2-1.

Quantity	Thermal System	Electrical System
Potential	T	E
Flow	$\dot{Q}$	I
Resistance	R	R
Conductance	G	$\frac{1}{R}$
Capacitance	C	C
Ohm's Law	$\dot{Q} = GT$	$I = \frac{E}{R}$

Table 2-1. Thermal-Electrical System Analogy

The analogy between thermal and electrical systems allows the engineer to utilize the widely known basic laws such as Ohm's Law and Kirchhoff's Laws used for balancing networks. Numerical techniques used to solve the partial differential equations describing such systems have been conveniently adapted to computer solutions, thus enabling the engineer to readily compute temperature distributions and gradients of complex physical thermal networks.

Thermal analyzer computer programs have been developed which require the user to define a thermal network of the system analogous to an electrical circuit. The network components are input into the computer and pre-programmed routines perform the transient or steady state solutions.

This section discusses the development of a thermal network and the numerical techniques for solving this network.

2.2 Modelling Elements

2.2.1 Nodes

2.2.1.1 Concepts

In order to develop a thermal network and apply numerical techniques to its solution, it is necessary to subdivide the thermal system into a number of finite subvolumes called nodes. The thermal properties of each node are considered to be concentrated at the central nodal point of each subvolume. Each node represents two thermal network elements, a temperature (potential) and a capacitance (thermal mass) as shown in Figure 2.1.

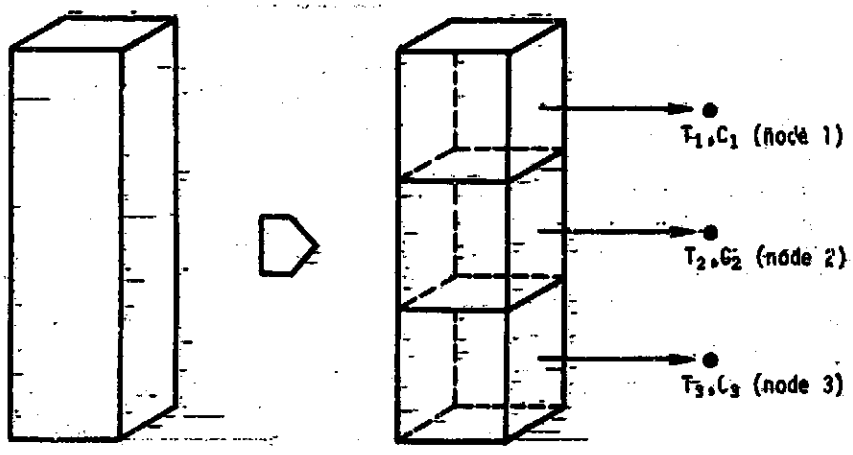

Figure 2-1. Nodalization

The temperature, T, assigned to a node represents the average mass temperature of the subvolume. The capacitance, C, assigned to a node is computed from the thermophysical properties of the subvolume material evaluated at the temperature of the node and is assumed to be concentrated at the nodal center of the subvolume. Because a node represents a lumping of parameters to a single point in space, the temperature distribution through the subvolume implied by the nodal temperature is linear as shown in Figure 2.2c and not a step function as illustrated in Figure 2.2b.

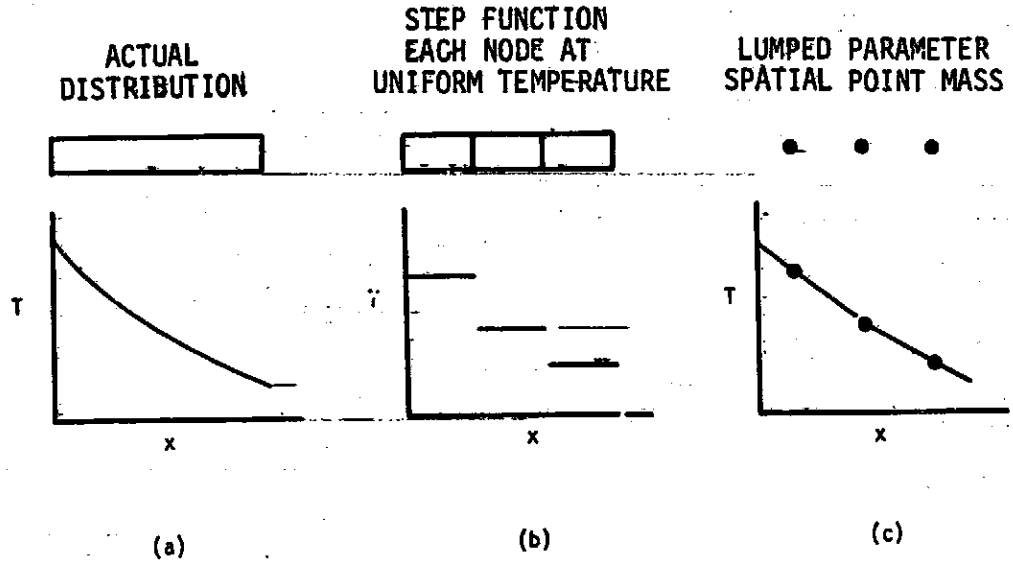

Figure 2.2. Temperature Distributions

In a homogeneous material, the temperature at a point other than the nodal point may be approximated by interpolation between adjacent nodal points where the temperatures are known.

The error introduced by dividing a system into finite size nodes rather than volumes dx^3 where dx approaches zero is dependent on numerous considerations: Material thermal properties, boundary conditions, node size, node center placement, and time increment of transient calculations. The techniques for proper nodalization to minimize the error will be discussed in a later section.

2.2.1.2 Node Types

To this point only nodes which represent subvolumes with a finite thermal mass (capacitance) have been discussed. In many instances, two other types of nodes are required to define a thermal network. They are nodes having a zero capacitance or an infinite capacitance. Thermal analyzers such as SINDA usually give the three types of nodes particular names as follows:

Node Type	Name
Finite Capacitance	Diffusion
Zero Capacitance	Arithmetic
Infinite Capacitance	Boundary

The diffusion node has a finite capacitance and is used to represent normal material nodalization. It is characterized by a gain or loss of potential energy which depends on the capacitance value, the net heat flow into the node, and the time over which the heat is flowing. Mathematically, a diffusion node is defined by the expression:

$$\Sigma\dot{Q} - \frac{C\Delta T}{t} = 0$$

The arithmetic node (zero capacitance) is a physically unreal quantity, however, its effective use with numerical solutions can often be helpful in interpreting results in such applications as surface temperatures, bondline temperatures, and node coupling temperatures. It also finds use in representing thermal system elements which have small capacitance values in comparison to the large majority of the other nodes in the system which results in computer run time reduction with minor changes in overall accuracy. Examples of these could be small components such as bolts, films, or fillets; gaseous contents of small ducts or tubes; and low mass insulations. Arithmetic nodes should be few in number when contrasted to the total number of nodes in the network. The temperature of an arithmetic node responds instantaneously to its surroundings. Mathematically, an arithmetic node is defined by the expression:

$$\Sigma\dot{Q} = 0$$

The boundary node (infinite capacitance) is used to represent constant temperature sources within a thermal network. Common uses are: deep space sink temperature, recovery temperature, lunar surface temperature. In addition, a boundary node may be used to represent thermal system components such as the bulk propellant in a large tank which has a very large thermal mass (capacitance). Mathematically a boundary node is defined as:

$$T = \text{Constant}$$

2.2.1.3 Method of Nodalization

The placement of diffusion node centers and the choice of node shapes is dependent on several factors: (1) the points where temperatures are desired, (2) the expected temperature distribution, (3) physical reasonableness, and (4) the ease of computation. The actual size of the node is dependent on other considerations: (1) accuracy desired, (2) structural design, (3) computer storage capabilities, and (4) computer time required. Each factor, however, embodies other considerations. For example, to anticipate the expected temperature distribution one must draw heavily on Engineering Judgement as to the effects of the expected boundary conditions and associated material properties.

In general, the shape of a diffusion node is chosen to be a simple geometric figure whose areas and volume can be easily calculated. Irregularly shaped structural members may be approximated by simple shapes by employing assumptions that are consistent with the desired results. Node centers are assumed to be located at the mass centroids of the nodes. In some cases, nodal divisions are decided first, with the node center locations being thusly defined as a consequence. In these cases, nodal boundaries will usually lie along structural boundaries, and structural members will be divided in a symmetric and equal fashion. In other cases, output requirements will dictate the locations of node centers, with the nodal boundaries assigned as a consequence. These two approaches are illustrated in Figure 2-3. In the first case, Figure 2-3(a) it is desired to prepare a general model of the structure, but in the second case, Figure 2-3(b) it is desired to model the response of the two thermocouples located on the bond line between the two members.

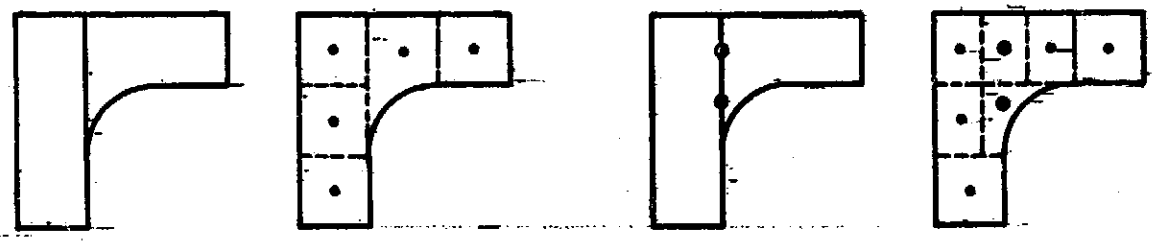

(a) General Node-Boundaries (b) Node Centers at Thermocouple Locations

Figure 2-3. Alternate Nodalization Methods

The above example alludes to a general desirability for rectangularly shaped nodes. This is true for the simple reason that it is easy to compute the areas and volumes required for the input calculations. Such simple nodal shapes are in keeping with current engineering practice. By contrast, Dusinberre (reference 1) suggested that nodalization be performed in such a manner that the paths of heat flow assumed a triangular pattern, as shown in Figure 2-4(a). The only drawback to this theoretically sound approach is that it remains for the engineer to compute the volumes of the irregular polygonal nodes which are the consequence of such a tact, as shown in Figure 2-4(b).

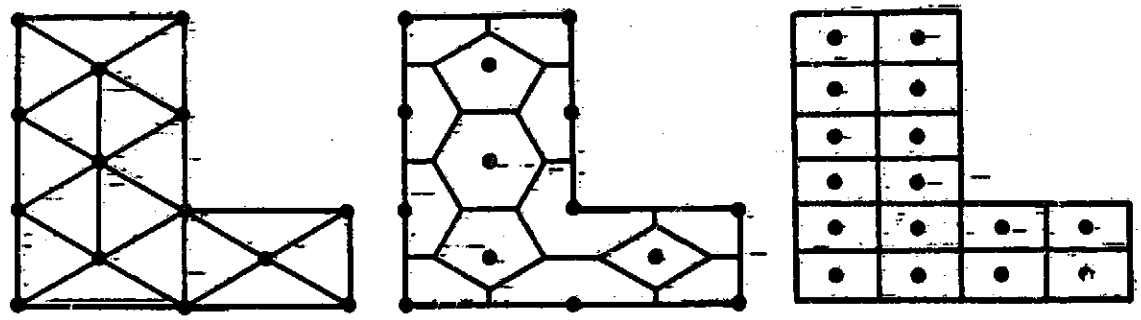

(a) Triangular Heat Flow Paths (b) Node Shapes Resulting from (a) (c) Simple Rectangular Nodalization

Figure 2-4. Polygonal Nodalization vs Rectangular Nodalization

Note how much simpler is the rectangular nodalization approach indicated in Figure 2-4(c). As might be expected, to achieve the same simplicity of calculation, circular structures are nodalized in pie-shaped wedges, annular rings, or a combination of the two, as shown in Figure 2-5.

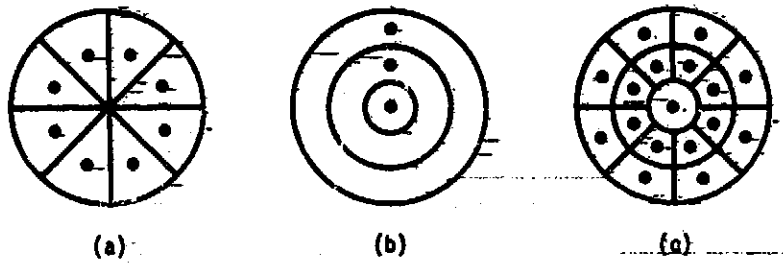

Figure 2-5. Nodalization of Circular Elements

Boundary nodes are used to define points, lines, or surfaces of constant temperature in one, two, or three dimensional models, respectively. The physical location of a boundary node is determined solely by the conduction paths connected to it. A single boundary node may be used to model all boundaries which are at the same temperature. This point is illustrated in Figure 2-6 which shows that the indicated boundary node will suffice as a model of the entire, constant temperature edge of the structure (in this case, at 100°F).

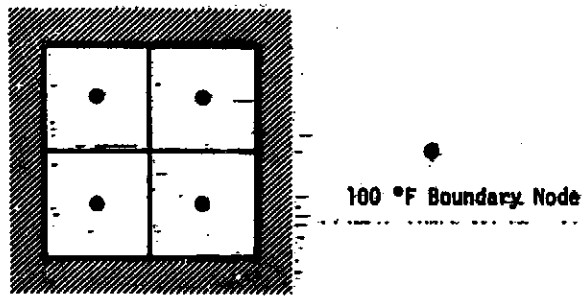

Figure 2-6. Sample Boundary Node

Arithmetic nodes have a number of uses which are consequences of the fact that such nodes serve as an engineering model of the proverbial "wafer of thickness dx, where dx approaches zero". A typical application lies in the modeling of exterior surfaces of reentry vehicles which are often subjected to severe, rapidly changing, boundary conditions. In the physical system, the surface temperature remains very close to radiation equilibrium with the surface heating rate, indicating that this system can be accurately simulated by the use of a surface arithmetic node. This application is illustrated in Figure 2-7.

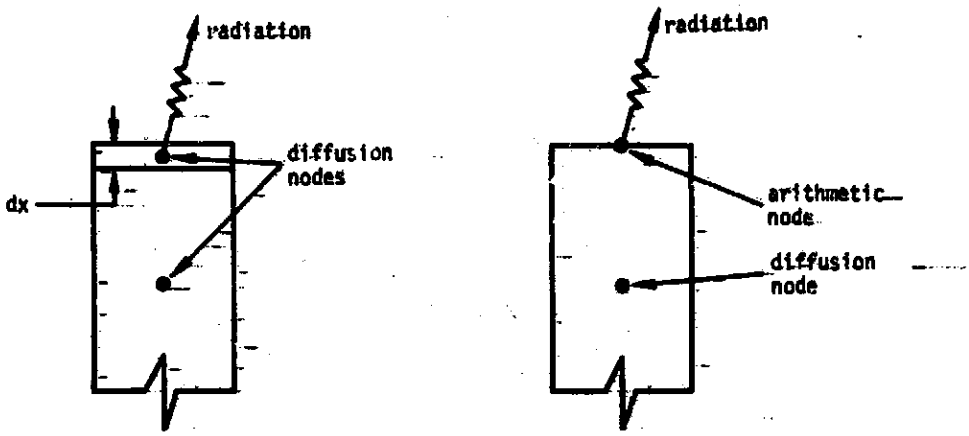

Figure 2-7. Use of Arithmetic Nodes to Model Surfaces

The case where heat flows from a surface by conduction is usually one in which two structures are bonded together and a bondline temperature is sought. When the structures are homogeneous, a bondline temperature may be established by simple linear interpolation between the nearest node centers. When the materials are dissimilar, it is more appropriate to use an arithmetic node at the bondline, leaving to the computer the process of performing a conductance weighted average of the adjoining diffusion node temperature which, in essence, is the result of finding the steady state (heat in = heat out) temperature for an arithmetic node.

Arithmetic nodes may also be used advantageously in place of diffusion nodes which have a capacitance that is small when compared to the great majority of nodes in the system. This often occurs when modeling a small quantity of gas in a tube or other enclosure, or when modeling small structural parts, such as wires, bolts, fillets, films, and sheets, where detailed temperatures are desired (which precludes lumping such items along with larger nearby nodes). The correct use of arithmetic nodes in these cases generally results in a considerable saving of computer time when the model is processed.

2.2.1.4 Computational Methods - Nodes

In developing a thermal network, computations with respect to nodes are generally limited to calculating the capacitance of diffusion nodes. The following formula is used:

$$C = \rho \cdot V \cdot C_p$$

where:

C = thermal capacitance - BTU/°F

ρ = density - LB/FT^3

V = volume - FT^3

C_p = specific heat - BTU/LB-°F

The specific heat (C_p) and the density (ρ) of materials may vary with temperature. The necessity to utilize temperature dependent properties for an analysis depends on the degree with which the properties vary and the temperature range over which the capacitance of the material will be calculated. Most thermal analyzers can accommodate temperature varying thermal properties.

The use of arithmetic nodes may also require some computations. Replacement of small capacitance diffusion nodes with an arithmetic node must be preceded by computations to verify that the capacitance-conductor effects are such that the node in question will essentially reach steady state temperatures during the time step required by the larger nodes. The use of an arithmetic node to predict surface temperatures where surface radiation or very high heating rates are involved requires careful analysis to insure the stability of the arithmetic node. Stability criteria and solution techniques are discussed in section 2.3. From this section, it can be seen that solution techniques using linearized "last pass" temperature values may require the use of analyzer control constants to restrict the maximum node temperature change or computation time step. The engineer must further be cautioned against using coupled arithmetic nodes without a complete understanding of the implications and required analyzer control constants used to insure a valid solution.

2.2.2 Conductors

2.2.2.1 Concepts

Conductors are the thermal math modeling network elements which are used to represent the heat flow paths through which energy is transferred from one node to another node. Figure 2-8 illustrates the element node temperatures (T), capacitances (C) and conductors (G) which comprise a thermal network.

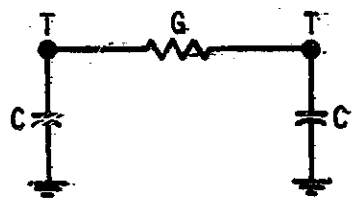

Figure 2-8. Thermal Network Elements

2.2.2.2 Types of Conductors

The three processes by which heat flows from a region of higher temperature to a region of lower temperature are conduction, convection, and radiation. Conduction is the process by which heat flows within a medium or between different mediums in direct physical contact. The energy is transmitted by molecular communication. Figure 2-9 illustrates conduction conductors.

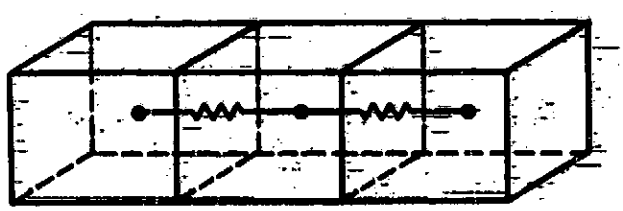

Figure 2-9. Conduction Conductor

Convection is the process of energy transport by combined action of heat conduction, energy storage, and mixing motion. Heat will flow by conduction from a surface to adjacent particles of fluid; then the fluid particles will

move to a region of lower temperature where they will mix with, and transfer a part of their energy to, other fluid particles. The energy is actually stored in the fluid particles and is carried as a result of their mass motion. Figure 2-10 illustrates the convection conductor.

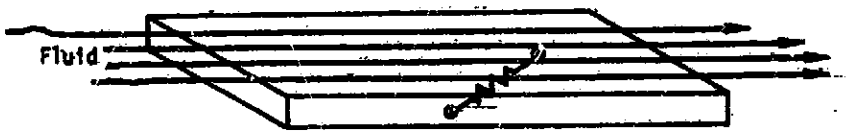

Figure 2-10. Convection Conductor

Conductors which represent conduction or convection paths are referred to as linear conductors because the heat flow rate is a function of the temperature difference between nodal temperatures to the first power.

$$\dot{Q} = G\,(T_i - T_j)$$

Radiation is the process by which heat flows between two bodies when the bodies are separated in space. Energy is transferred through electromagnetic wave phenomena. Radiation conductors are termed non-linear because the heat flow between two surfaces by radiation is a function of the difference of the fourth powers of the surface temperatures.

$$\dot{Q} = G\,(T_i^4 - T_j^4)$$

Figure 2-11 illustrates the radiation conductor.

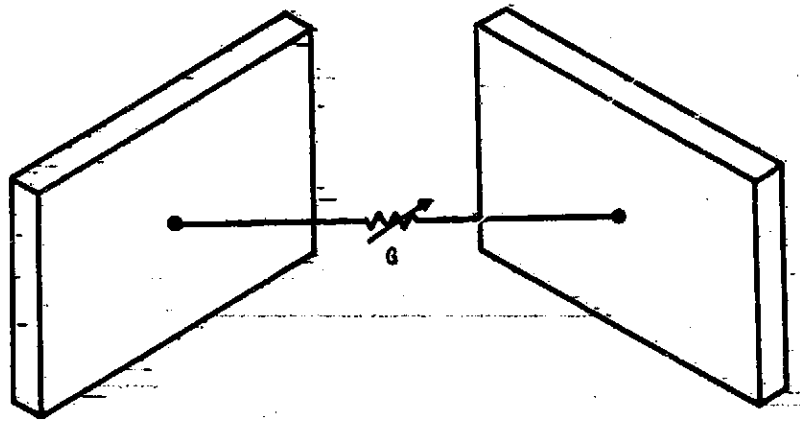

Figure 2-11. Radiation Conductor

Fluid flow thermal systems may also be simulated by thermal modeling. Energy stored in the thermal mass (capacitance) of a fluid lump (node) is transferred from one point to another by the movement of the fluid mass. This type of conductor is generally referred to as a mass flow conductor and is illustrated in Figure 2-12. The mass flow conductor is also linear

$$\bar{Q} = G\,(T_i - T_j)$$

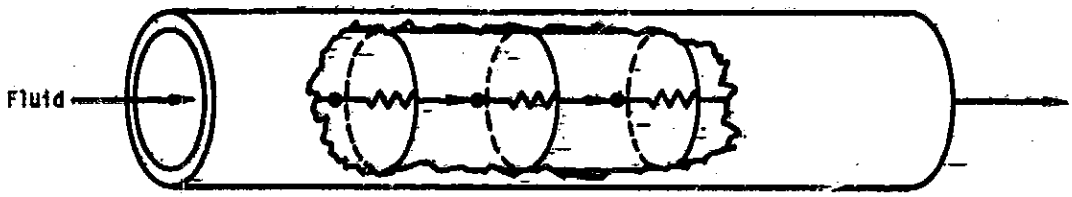

Figure 2-12. Mass Flow Conductors

2.2.2.3 Computational Methods - Conduction Conductors

Conduction conductors are computed from the equation:

$$G = \frac{kA}{L}$$

where:

G = thermal conductance - BTU/HR-°F

k = thermal conductivity - BTU/HR-FT-°F

A = cross sectional area through which heat flows - FT^2

L = length between adjoining nodes - FT

The thermal conductivity (k) of materials may vary with temperature or other influencing factors within the system; the cross-sectional area through which the heat flows (A) and length between node centers (L) are determined by the size and shape of the adjoining nodes. As with the capacitance calculations, the necessity to use temperature dependent properties depends on the degree with which the conductivity changes over the temperature range expected during the analysis.

2.2.2.3.1 Rectangular Nodes

The length, L, of the heat flow path, used for conduction conductance calculations for rectangular nodes is the distance between node centers, and the area, A, to be used is the cross-sectional area perpendicular to the line joining the node centers. The convention is depicted in Figure 2-13.

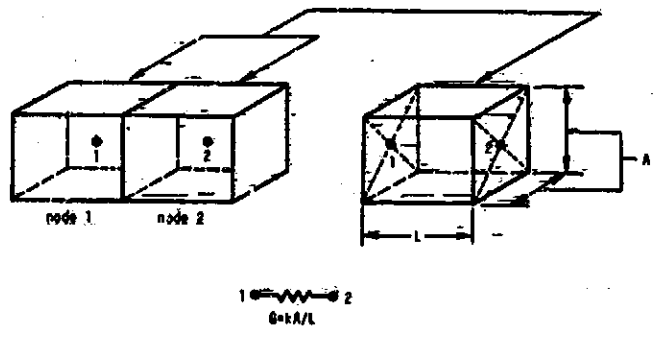

Figure 2-13. Simple Conductor Representing a Heat Flow Path through Material

2.2.2.3.2 Circular Sections

For conductors between nodes which are circular sections, the conventions shown in Figure 2-14 should be used:

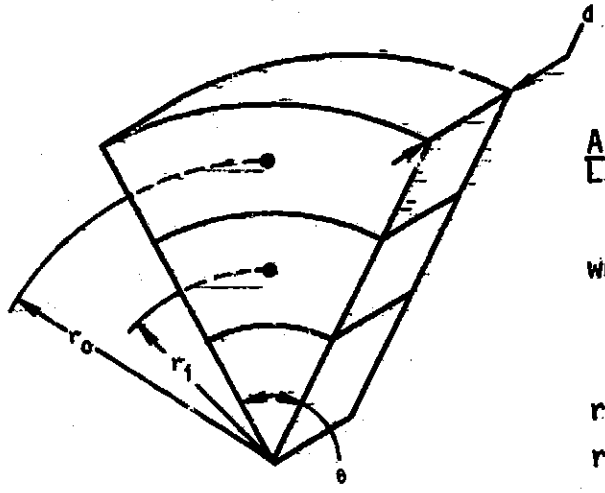

$$\frac{A}{L} = \frac{\theta d}{\ln(r_o/r_i)}$$

where:

θ - radians

d - FT

r_o - consistent units with r_i

r_i - consistent units with r_o

Figure 2-14. Area and Length Equivalents for Circular Section Nodes

2.2.2.3.3 Parallel Conductors

Two or more parallel conduction paths between nodes may be summed to create one conductor value by the following equation:

$$G_T = G_1 + G_2 + \ldots G_n$$

This may be helpful in computing an equivalent conductor between two nodes as illustrated in Figure 2.15.

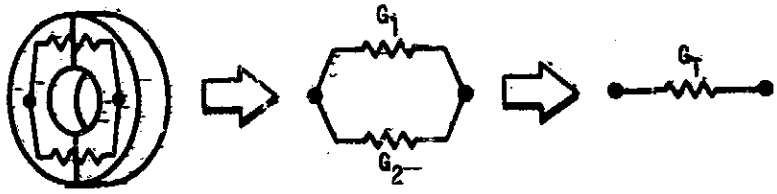

$$G_T = G_1 + G_2$$

Figure 2.15. Parallel Conductor Flow Paths

2.2.2.3.4 Series Conductors

Two or more series conduction paths between nodes may be combined to create one conductor value by the following equation:

$$\frac{1}{G_T} = \frac{1}{G_1} + \frac{1}{G_2} + \cdots \qquad G_T = \frac{1}{\frac{1}{G_1} + \frac{1}{G_2} + \cdots \frac{1}{G_n}}$$

This may be helpful in computing the conductors between two dissimilar shaped or dissimilar material nodes as shown in Figure 2.16.

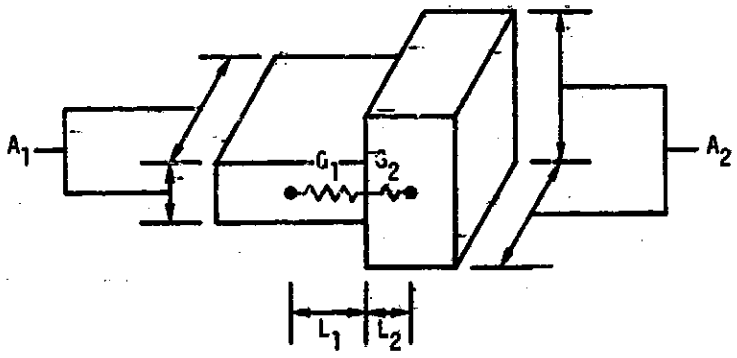

$$G_1 = \frac{k_1 A_1}{L_1}$$

$$G_2 = \frac{k_2 A_2}{L_2}$$

$$G_T = \frac{1}{\frac{1}{G_1} + \frac{1}{G_2}} = \frac{G_1 G_2}{G_1 + G_2}$$

Figure 2.16. Series Conductor Paths

2.2.2.4 Computational Methods – Convection Conductors

Convection conductors are computed from the expression:

$$G = hA$$

where:

G = thermal conductance - BTU/HR-°F

h = convective heat transfer coefficient - BTU/HR-FT^2-°F

A = surface area in contact with the fluid - FT^2

G is the product of the average unit thermal convective conductance h (convective heat transfer or film coefficient) and the nodal surface area A in contact with the fluid. However, h is a complicated function of fluid flow, the thermal properties of the fluid medium, and the geometry of the system.

Since the convective process of heat transfer is so closely linked to fluid motion, it is first required to establish whether the fluid flow is laminar or turbulent. In laminar flow the fluid moves in layers and the fluid particles follow a smooth and continuous path. Heat is transferred only by molecular conduction within the fluid as well as at the interface between the fluid and the surface. In turbulent flow the path of the fluid particles is irregular, and although the general trend of the motion is in one direction, eddies or mixing currents exist. In addition to the conduction mechanism being modified, increased heat transfer occurs in turbulent flow when energy is carried by fluid particles across flow streamlines and mixes with other particles of the fluid.

In addition to knowing whether the fluid motion is laminar or turbulent, it is necessary to know the process by which the motion was induced. When the heat flows between the fluid and the surface as a result of fluid motion caused by differences in fluid density resulting from temperature gradients in the fluid, the heat transfer mechanism is called free or natural convection. When the motion is caused by some external agency, such as a pump or blower, the heat transfer mechanism is called forced convention.

The following table illustrates typical values of average heat transfer coefficients encountered in engineering practice.

Convective Medium	Convective Heat Transfer Coefficient h - BTU/HR-FT^2-°F
Air, Free Convection	1-5
Air, Forced Convection	5-50
Oil, Forced Convection	10-300
Water, Forced Convection	50-2000
Water, Boiling	500-10,000
Steam, Condensing	1000-20,000

Table 2-2. Order of Magnitude of Conveetive Heat Transfer Coefficients

Equations for the computation of convective heat transfer coefficients will be divided into three categories: natural conveetion, forced convection in tubes or ducts, and forced convection over exterior surfaces. The equations presented for the calculation of convective film coefficients are the most generally used expressions. Others are available and are applicable for many specific thermal problems or analyse,. It should be remembered that the predicted values for h are only approximate. The accuracy of the heat-transfer coefficient calculated from any available equation or graph may be no better than 30 percent.

2.2.2.4.1 Combined Natural and Forced Convection

In cases where both natural and forced convection are combined, it is left to the engineer to decide which heat transfer phenomena is significant and utilize the proper equations to compute the effective film coefficient (h). The following determinations should be helpful:

1) Calculate the Grashof number (Gr)

$$Gr = \frac{\rho^2 \, g \, \beta \, (T - T_\infty) \, L^3}{\mu^2}$$

where:

Gr = Grashof number - dimensionless

g = gravity constant - 4.17×10^8 FT/HR^2

β = coefficient of volumetric expansion @ film temperature - 1/°R

T = temperature of the body surface - °F

T_∞ = temperature of the surrounding medium - °F

L = length of flow path - FT

μ = fluid viscosity - LB/HR-FT

2) Calculate the Reynolds number (Re)

$$Re = \frac{U \rho L}{\mu}$$

where:

Re = Reynolds number - dimensionless

U = fluid velocity - FT/HR

ρ = fluid density - LB/FT^3

L = length of flow path - FT

μ = fluid viscosity - LB/HR-FT

3) If $Gr \leq 0.225\ Re^2$ the effect of natural convection on the average heat transfer coefficient for pure forced convection is less than 5%

4) If $Gr > 10.0\ Re^2$ forced convection has negligible effect on natural convection

5) In the region where both free and forced convection effects are of the same order of magnitude, heat transfer is increased by buoyancy effects acting in the direction of flow and decreased when acting in the opposite direction.

6) In cases where it is doubtful whether forced or free convection flow applies, the heat transfer coefficient is generally calculated by using forced and free convection relations separately and the larger one is used. The accuracy of this rule of thumb is estimated to be about 25%.

2.2.2.4.2. Natural Convection Equations

Natural convection occurs when fluid is set in motion as a result of density differences due to temperature variations in the fluid. A great deal of material has been published on heat transfer coefficients, resulting in many techniques with a wide variety of results, leaving the "occasional user" of the information easily confused. Presented herein is a wide variety of applications condensed into a small number of groups. The initial data was obtained from the Oil and Gas Journal. Equations used are the ones which appear to have the widest acceptance for the particular set of conditions involved.

Correlations of natural convection heat transfer usually take the form:

$$h = K\,(Gr\ Pr)^n$$

where:

h = heat transfer coefficient
K = an empirical constant
Pr = Prandtl number
Gr = Grashof number
n = an empirical exponent

To apply the above equations to an actual problem solution, the following steps should be performed:

1). Calculate the product of the Prandtl and Grashof numbers

$$Gr \cdot Pr = \frac{\rho^2\ \beta\ C_p\ g\ \Delta T\ L^3}{\mu\ k}$$

where:

k = thermal conductivity @ film temperature - BTU/FT^2-HR-°F-FT

ρ = density @ film temperature - LB/FT^3

β = coefficient of volumetric expansion. @ film temperature - 1/°R

g = gravity constant - 4.17×10^8 FT/HR^2

C_p = specific heat @ film temperature - BTU/LB-°F

μ = viscosity @ film temperature - LB/FT-HR

L = height or length of surface - FT

ΔT = temperature difference between the wall and and fluid - °F

Film temperature = $\frac{T_{wall} + T_{fluid}}{2}$ - °F

2) If $10^3 < Gr\ Pr < 10^9$ assume flow is laminar and go to Step 3.

If $Gr\ Pr > 10^9$ assume flow is turbulent and go to Step 4.

3) Laminar Flow

$$h = C_1 \frac{k}{L} (Gr\ Pr)^{1/4}$$

where:

h = heat transfer coefficient - BTU/FT^2-HR-°F

k = thermal conductivity at film temperature - BTU/FT-HR-°F

L = height or length of surface - FT

Gr Pr = Product of Grashof and Prandtl numbers from above - dimensionless

C_1 is dependent on the geometry of the system and can be determined from Figure 2-17

Film temperature = $\frac{T_{wall} + T_{fluid}}{2}$ - °F

4) Turbulent Flow

$$h = C_1 \frac{k}{L} (Gr \cdot Pr)^{1/3}$$

where:

h = heat transfer coefficient - BTU/FT^2-HR-°F

k = thermal conductivity at film temperature - BTU/FT-HR-°F

L = height or length of surface - FT

Gr Pr = Product of Grashof and Prandtl numbers from above - dimensionless

C_1 is dependent on the geometry of the system and can be determined from Figure 2-18

Film temperature = $\frac{T_{wall} + T_{fluid}}{2}$ - °F

LAMINAR FLOW

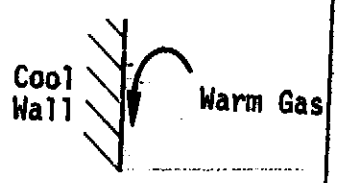

Short Wall < 2 ft

C_1 = 0.548

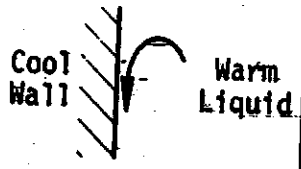

Short Wall < 0.15 ft

C_1 = 0.548

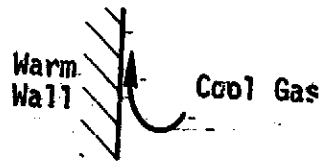

Short Wall < 2 ft

C_1 = 0.548

Short Wall < 0.15 ft

C_1 = 0.55

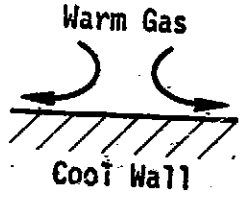

Small Wall < 2 ft sect

C_1 = 0.35

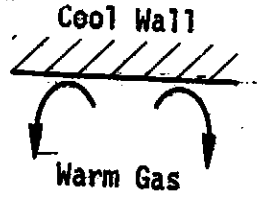

Small Wall < 2 ft sect

C_1 = 0.71

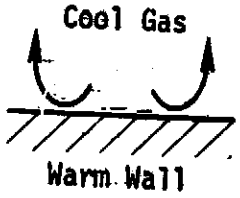

Small Wall < 2 ft sect

C_1 = 0.71

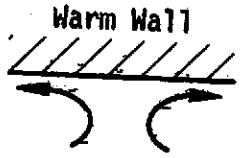

Small Wall < 2 ft sect

C_1 = 0.35

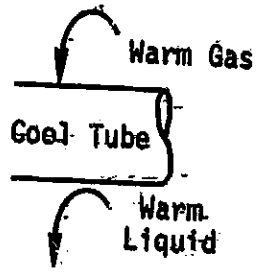

Small Tube: D < 1 in

C_1 = 0.53 Sub D for L

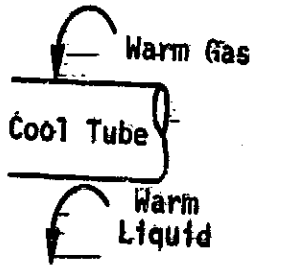

Small Tube: 1 in < D < 4 in

C_1 = 0.47 Sub D for L

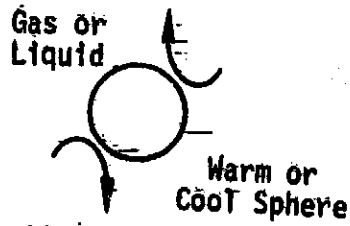

Small Diameter

Liquid: R < 0.15 ft

Gas: R < 0.50 ft

C_1 = 0.63 Sub R for L

Figure 2-17. Empirical Constants for Natural Convection - Laminar Flow

TURBULENT FLOW

Long Wall > 2 ft

$C_1 = 0.13$

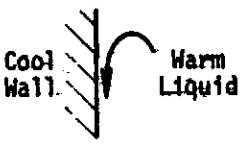

Long Wall > 0.15 ft

$C_1 = 0.13$

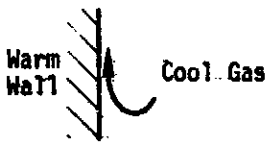

Long Wall > 2 ft

$C_1 = 0.13$

Long Wall > 0.15 ft

$C_1 = 0.13$

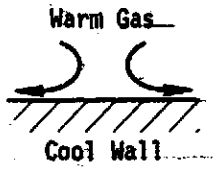

Large Wall > 3 ft^2

$C_1 = 0.08$

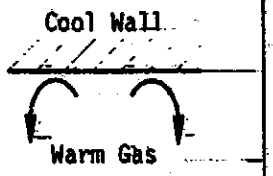

Large Wall > 3 ft^2

$C_1 = 0.162$

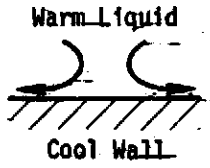

Large Wall > 0.25 ft^2

$C_1 = 0.08$

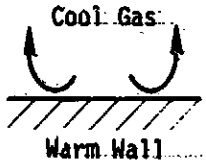

Large Wall > 3 ft^2

$C_1 = 0.162$

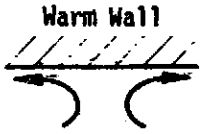

Large Wall > 3 ft^2

$C_1 = 0.08$

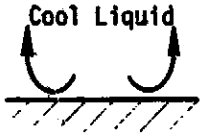

Large Wall > 3 ft^2

$C_1 = 0.162$

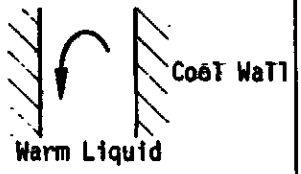

$C_1 = 0.128$

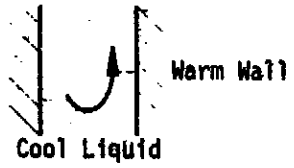

$C_1 = 0.128$

$C_1 = 0.128$

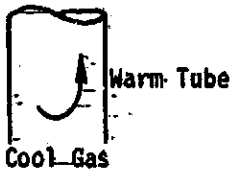

$C_1 = 0.128$

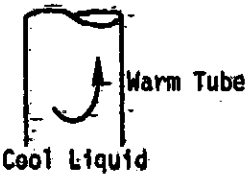

$C_1 = 0.128$

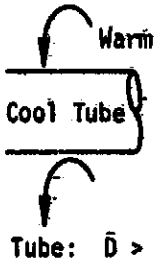

Large Tube: D > 6 in

$C_1 = 0.11$ Sub D for L

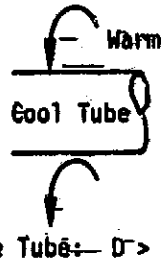

Large Tube: D > 6 in

$C_1 = 0.11$ Sub D for L

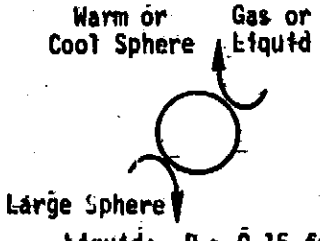

Liquid: R > 0.15 ft
Gas: R > 0.50 ft

$C_1 = 0.15$ Sub R for L

Figure 2-18. Empirical Constants for Natural Convection - Turbulent Flow

2.2.2.4.3 Forced Convection In Tubes and Ducts

To apply the empirical relationships for forced convection heat transfer coefficients in tubes and ducts, the following steps should be performed. Comments on thermophysical property determination and entrance effects are included at the end of the section.

1) Calculate the hydraulic diameter, D_H, which is defined as:

$$D_H = 4 \frac{\text{flow cross-sectional area}}{\text{wetted perimeter}}$$

The hydraulic diameter for some common shaped tubes or ducts is:

Round: $D_H = D$, where D is the diameter of the tube

Square: $D_H = L$ where L is the length of a side

Rectangle: $D_H = \frac{2ab}{a+b}$, where a and b are the lengths of the sides

Elliptical: $D_H = ab\sqrt{\frac{2}{a^2 + b^2}}$, where a and b are major and minor axes

Annular: $D_H = D_o - D_i$, where D_o is the outer tube diameter
D_i is the inner tube diameter

2) Compute the Reynolds number, Re, from the following equation:

$$Re = \frac{U D_H \rho}{\mu}$$

where:

D_H = hydraulic diameter, defined above - FT
U = velocity - FT/HR
ρ = density - LB/FT^3
μ = viscosity - LB/FT-HR

3) If Re < 2100 the flow can be considered laminar, go to step 4
If Re > 10,000 the flow can be considered turbulent, go to step 5
If 2100 < Re > 10,000 the flow can be considered transitional, go to step 6

4) Laminar Flow

$$h = 1.86\ k\left(Re\ Pr\frac{1}{D_H^2\ L}\right)^{1/3}$$

$h = 3.66\frac{k}{D}$ is a minimum for laminar flow in long tubes

for very short tubes

$$\left(\frac{L}{D_H} < .005\ Re\right) :=$$

$$h = \frac{Re\ Pr\ k}{4L}\ln\left[\frac{1}{1-\left(\frac{2.654}{Pr^{.167}\left(Re\ Pr\ D_H/L\right)^{.5}}\right)}\right]$$

where:

h = convective heat transfer coefficient - BTU/FT^2-HR-°F

Re = Reynolds number from step 2 - dimensionless

D_H = hydraulic diameter - from step 1 - FT

L = tube or duct length - FT

D = tube or duct diameter - FT

Pr = Prandtl number = $\frac{C_p\ \mu}{k}$ - dimensionless

C_p = specific heat - BTU/LB-°F

k = thermal conductivity - BTU/FT-HR-°F

μ = viscosity - LB/FT-HR

5) Turbulent Flow

$$h = 0.023 \frac{k}{D_H} Re^{.8} Pr^{.33}$$

where:

h = heat transfer coefficient - BTU/FT^2-HR-°F

k = thermal conductivity - BTU/FT-HR-°F

D_H = hydraulic diameter - from step 1 - FT

Re = Reynolds number - from step 2 -- dimensionless

Pr = Prandtl number = $\frac{C_p \mu}{k}$ - dimensionless

C_p = specific heat - BTU/LB-°F

μ = viscosity - LB/FT-HR

6) Transition Flow

$$h = C_1 C_p U \rho Pr^{1/3} \left(\frac{\mu_b}{\mu_s}\right)^{.14}$$

where:

h = heat transfer coefficient - BTU/FT^2-HR-°F

C_p = specific heat - BTU/LB-°F

U = velocity - FT/HR

ρ = density - LB/FT^3

Pr = Prandtl number = $\frac{C_p \mu}{k}$ - dimensionless

μ = viscosity evaluated at the average film temperature - LB/FT-HR

μ_b = viscosity evaluated at the bulk fluid temperature - LB/FT-HR

μ_s = viscosity evaluated at the surface temperature - LB/FT-HR

k = thermal conductivity - BTU/FT-HR-°F

C_1 = a function of Re and can be determined from Figure 2-19

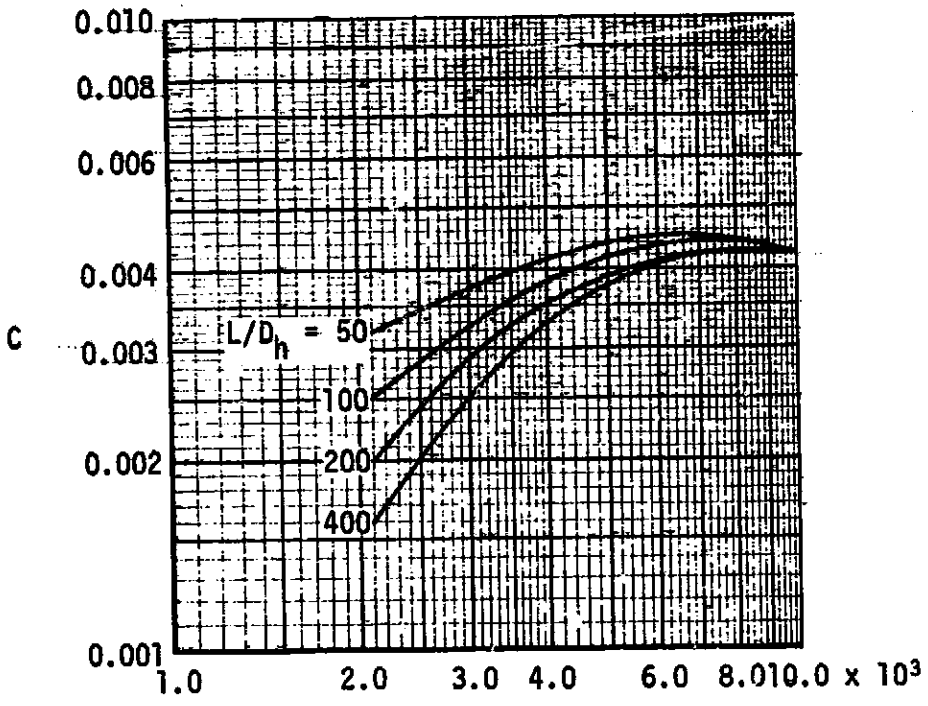

Figure 2-19. Empirical Constant for Forced Convection Transition Flow in Tubes and Ducts

Thermophysical Properties

Because the film coefficient (h) is a function of the thermophysical properties of the fluid, it is important to account for any significant variation in the properties as a result of the temperature of the fluid. For liquids, generally only the temperature dependence of the viscosity (μ) is of major importance. For gases, the other properties density (ρ), conductivity (k) and specific heat (C_p) usually vary significantly. It is recommended that all of the properties except C_p be evaluated at the average film temperature of the fluid T_f defined as:

$$T_f = 0.5\ (T_s + T_b)$$ where T_s = surface temperature
T_b = fluid bulk temperature

C_p should be evaluated at the fluid bulk temperature.

All of the above equations, with the exception of the one for computing h for laminar flow in very short tubes, ignore entrance effects on the film coefficient. The importance of entrance effects depends on the fluid flow condition and the length (L)/hydraulic diameter (D_H) of the tube or duct. Entrance effects are appreciable where:

For laminar flow $\frac{L}{D_H} < 50$

For turbulent flow $\frac{L}{D_H} < 10$

In general, entrance effects increase the effective film coefficient. The local heat transfer coefficient (h_x) divided by the free stream heat transfer coefficient (h_∞) approaches 1 as $\frac{L}{D}$ increases. If the detail of an analysis requires the consideration of entrance effects on the convection coefficient, literary research may be helpful in finding an equation approximating the effect. An example of entrance effect correction is as follows: consider turbulent flow in short circular tubes where ($2 < L/D < 60$), the effective film coefficient can be approximated by:

$$h_E = h + h\left(\frac{D}{L}\right)^{.7} \quad \text{where } 2 < L/D < 20$$

$$h_E = h + h\left(\frac{6D}{L}\right) \quad \text{where } 20 \leq L/D < 60$$

where:

h_E = effective film coefficient corrected for entrance effects - same units as h

h = turbulent film coefficient calculated from step 5

D = tube diameter - units consistent with L

L = tube length - units consistent with D

2.2.2.4.4 Forced Convection Over Flat Plates

Emperical relationships for forced convection over the exterior surface of a flat plate are given for both the entire length (L) of the plate and at any intermediate length (x). Equations for both locations are given in stepwise fashion:

1) Calculate the Reynolds number Re

$$Re_x = \frac{U_\infty \rho x}{\mu}$$

$$Re_L = \frac{U_\infty \rho L}{\mu}$$

where:

U_∞ = free stream velocity - FT/HR

ρ = fluid density - LB/FT^3

μ = fluid viscosity - LB/FT-HR

x = intermediate plate length - FT

L = total plate length - FT

2) If $Re < 5 \times 10^5$ flow is laminar, go to step 3
If $Re > 5 \times 10^5$ flow is turbulent, go to step 4

3) Laminar heat transfer coefficient (h)

Evaluated at x, $h = .332 \frac{k}{x} Re_x^{1/2} Pr^{1/3}$

Average value for plate with length L,

$$h = .664 \frac{k}{L} Re_L^{1/2} Pr^{1/3}$$

where:

h = convective heat transfer coefficient - $BTU/HR\text{-}FT^2\text{-}^\circ F$

k = thermal conductivity - $BTU/HR\text{-}FT\text{-}^\circ F$

x = intermediate plate length - FT

L = total plate length - FT

Re = Reynolds number from step 1 - dimensionless

Pr = Prandtl number = $\frac{C_p \mu}{k}$ - dimensionless

μ = viscosity - LB/FT-HR

4) Turbulent heat transfer coefficient (h)

Evaluated at x, $h = 0.0288 \frac{k}{x} Re_x^{.8} Pr^{1/3}$

Average value for plate with length L,

$$h = 0.036 \frac{k}{L} Re_L^{.8} Pr^{1/3}$$

where:

h = convective heat transfer coefficient - BTU/HR-FT^2-°F

k = thermal conductivity - BTU/HR-FT-°F

x = intermediate plate length - FT

L = total plate length - FT

Re = Reynolds number from step 1 - dimensionless

Pr = Prandtl number = $\frac{C_p \mu}{k}$ - dimensionless

μ = viscosity - LB/FT-HR

2.2.2.4.5 Forced Convection Over Cylinders

Empirical relationships for flow over cylinders are given for the stagnation point, forward portion of the cylinder, and for laminar flow over the total cylinder.

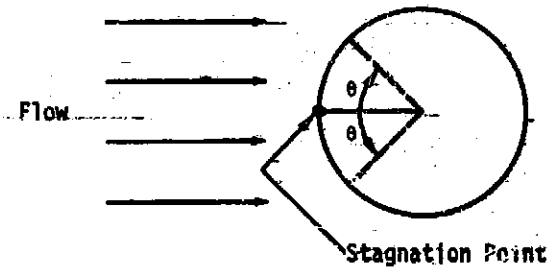

Figure 2-20. Flow Over Cylinders

Stagnation Point

$$h = C_1 \frac{k}{D} \sqrt{U_\infty \frac{D\rho}{\mu}}$$

where:

h = convective heat transfer coefficient - BTU/FT^2-HR-°F

k = thermal conductivity - BTU/FT-HR-°F

U_∞ = free stream velocity - FT/HR

D = cylinder diameter - FT

ρ = density - LB/FT^3

μ = viscosity - LB/FT-HR

C_1 = is a function of Pr = $\frac{C_p \mu}{k}$ and can be approximated from Figure 2-21

C_p = specific heat - BTU/LB-°F

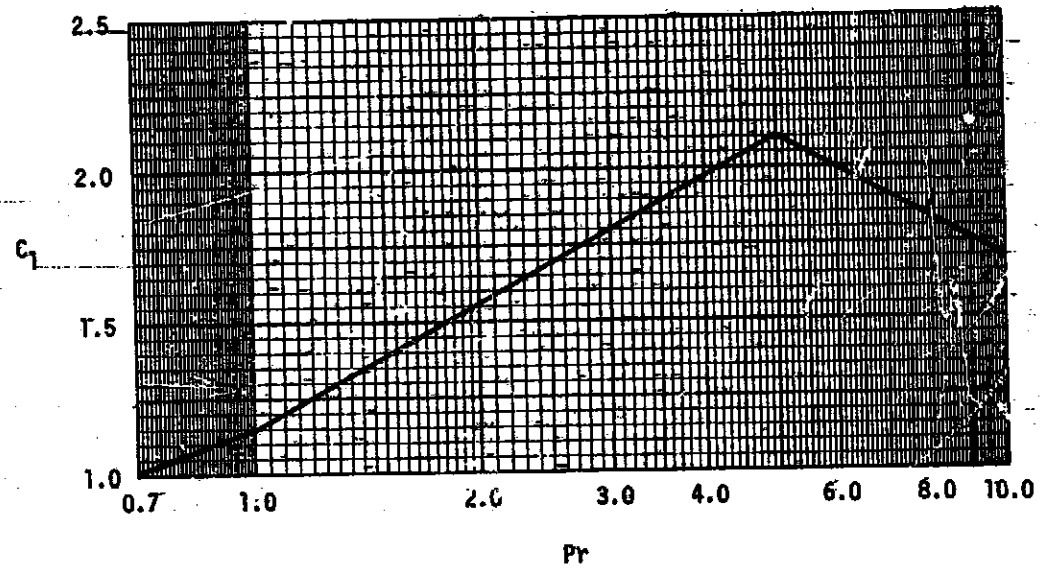

Figure 2-21. Empirical Constant for Cylinder Stagnation Point

Forward portion of cylinder where ($0° < \theta < 80°$) (see Figure 2-20)

$$h_\theta = 1.14 \frac{k}{D} \left(\frac{U_\infty D \rho}{\mu} \right)^{.5} Pr^{.4} \left[1 - \left(\frac{\theta}{90} \right)^3 \right]$$

where:

h = convective heat transfer coefficient - BTU/FT^2-HR-°F

k = thermal conductivity - BTU/FT-HR-°F

D = cylinder diameter - FT

U_∞ = free stream velocity - FT/HR

ρ = density - LB/FT^3

μ = viscosity - LB/FT-HR

Pr = Prandtl number = $\frac{C_p \mu}{k}$ - dimensionless

C_p = specific heat - BTU/LB-°F

θ = angle measured from the stagnation point - degrees

Average film coefficient for laminar flow over a cylinder

for a gas $$h = C \frac{k}{D} \left(\frac{U_\infty D \rho}{\mu} \right)^n$$

for a liquid $$h = 1.1\, C \frac{k}{D} \left(\frac{U_\infty D \rho}{\mu} \right)^n Pr^{.31}$$

where:

h = convective heat transfer coefficient - BTU/FT^2-HR-°F

k = thermal conductivity - BTU/FT-HR-°F

D = cylinder diameter - FT

U_∞ = free stream velocity - FT/HR

ρ = density - LB/FT^3

μ = viscosity - LB/FT-HR

Pr = Prandtl number - $\frac{C_p \mu}{k}$ - dimensionless

C_p = specific heat - BTU/LB-°F

C = empirical constant determined from Table 2-3 as a function of Reynolds number (Re) = $U_\infty \rho D/\mu$

n = empirical exponent determined from Table 2-3 as a function of Reynolds number (Re) = $U_\infty \rho D/\mu$

Re_D	C	n
0.4-4	0.891	0.330
4-40	0.821	0.385
40-4,000	0.615	0.466
4,000-40,000	0.174	0.618
40,000-400,000	0.0239	0.805

Table 2-3. Empirical Constants for Laminar Flow Over a Cylinder

Turbulence induced in the air upstream of the cylinder may increase h by as much as 50 percent.

2.2.2.4.6 Forced Convection Over Spheres

Empirical relationships for average value heat transfer coefficients for flow over spheres are given for gasses and liquid as outlined in the following steps:

1) Calculate Reynolds number $Re = U_\infty \rho D/\mu$

where:

U_∞ = free stream velocity – FT/HR

ρ = density - LB/FT^2

D = sphere diameter - FT

μ = viscosity - LB/FT-HR

2) For a gas where $(1 < Re < 25)$ use step 3
For a gas where $(25 < Re < 100{,}000)$ use step 4
For a liquid where $(1 < Re < 2{,}000)$ use step 5

3) Gas where $1 < Re < 25$

$$h = C_p U_\infty \rho_\infty \left(\frac{2.2}{Re} + \frac{0.48}{Re^{0.5}} \right)$$

where:

h = convective heat transfer coefficient - $BTU/FT^2\text{-}HR\text{-}°F$

C_p = specific heat - BTU/LB-°F

U_∞ = free-stream velocity – FT/HR

ρ_∞ = free stream density - LB/FT^3

Re = Reynolds number from step 1 - dimensionless

4) Gas where $25 < Re < 100{,}000$

$$h = 0.37 \frac{k}{D} \left(\frac{U_\infty \rho_\infty D}{\mu} \right)^{.6}$$

where:

h = convective heat transfer coefficient - BTU/FT^2-HR-°F

k = thermal conductivity - BTU/FT-HR-°F

D = sphere diameter - FT

U_∞ = free stream velocity - FT/HR

ρ_∞ = free stream density - LB/FT^3

μ = viscosity - LB/FT-HR

5) Liquid where $1 < Re < 2000$

$$h = \frac{k\ Pr^{.7}}{D}\left[0.97 + 0.68\left(\frac{U_\infty\ \rho_\infty\ D}{\mu}\right)^{.5}\right]$$

where:

h = convective heat transfer coefficient - BTU/FT^2-HR-°F

k = thermal conductivity - BTU/FT-HR-°F

Pr = Prandtl number = $\frac{C_p\ \mu}{k}$ - dimensionless

C_p = specific heat - BTU/LB-°F

μ = viscosity - LB/FT-HR

D = sphere diameter - FT

U_∞ = free stream velocity - FT/HR

ρ_∞ = free stream density - LB/FT^3

2.2.2.5 Computational Methods - Radiation Conductors

Most thermal analyzer computer programs linearize the radiation term prior to performing the heat balance at each time step. This operation simply amounts to factoring $(T_i^4 - T_j^4)$ into the following components $(T_i^3 + T_i T_j^2 + T_i^2 T_j + T_j^3)(T_i - T_j)$, the term $(T_i^3 + T_i T_j^2 + T_i^2 T_j + T_j^3)$ is evaluated by the computer each time pass using the current values of T_i and T_j. This quantity is then multiplied by the input value of the radiation conductor thus reducing the radiation equation to a linear form. The thermal engineer need only be concerned with the input value of the radiation conductor which takes the following form:

$G = \sigma \varepsilon F_{i-j} A_i$ for radiation to a black body

$G = \sigma \mathcal{F}_{i-j} A_i$ for radiation between grey surfaces

where:

G = input value for radiation conductors - BTU/HR-°R⁴

σ = Stephan-Boltzmann constant = $.1713 \times 10^{-12}$ - BTU/HR-FT²-°R⁴

ε = emittance - dimensionless

F_{i-j} = geometric configuration factor from surface i to surface j - dimensionless

A_i = area of surface i - FT²

$\mathcal{F}_{i-j}$ = grey body radiation factor - dimensionless

The emittance, ε, is a measure of how well a body can radiate energy as compared with a black body. Emittance is the ratio of the total emissive power of a real surface at temperature T to the total emissive power of a black surface at the same temperature. The emittances of various surfaces are a function of the material, surface condition, and temperature of a body. The surface of a body, and therefore the emittance, may be altered by polishing, roughing, painting, etc. The values of ε for most common materials and surface conditions have been measured at various temperatures and are presented in tables or graphs in many reference manuals. It is left to the engineer to determine the value of emittance to be used and whether the variation of ε with temperature is significant over the temperature range expected for the surface.

The geometric shape (configuration) factor from surface i to surface j, F_{i-j}, is the fraction of total radiated energy from surface i which is directly incident on surface j, assuming surface i to be emitting energy diffusely. F_{j-i} would be the fraction of total radiant energy from surface j which is intercepted by surface i. The configuration factors for finite regions of diffuse areas are related by:

$$A_i F_{i-j} = A_j F_{j-i}$$

The configuration factor, F_{i-j}, is a function of the geometry of the system only. Several computer programs have been developed to compute the shape factors between surfaces with complex geometries; however, form factors between some surfaces with simple geometries can be hand computed.

Figures 2.22 through 2.38 present configuration factors for various simple geometries. The use of these Figures and configuration factor algebra will allow the engineer to determine form factors for many simple radiation problems.

The following examples of configuration factor algebra should be helpful:

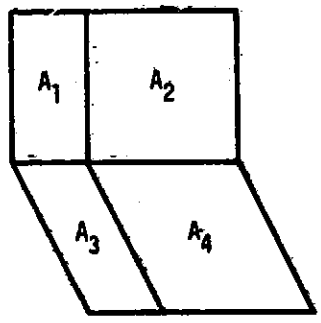

$A_1 F_{1-3} = A_3 F_{3-1}$

$A_1 F_{1-34} = A_1 F_{1-3} + A_1 F_{1-4}$

$A_{12} F_{12-34} = A_1 F_{1-34} + A_2 F_{2-34}$

$A_{12} F_{12-34} = A_1 F_{1-3} + A_1 F_{1-4} + A_2 F_{2-3} + A_2 F_{2-4}$

$A_1 F_{1-4} = A_3 F_{3-2}$ (symmetrically positioned)

Figure 2-22. Radiant - Interchange Configuration Factors† Point Sources

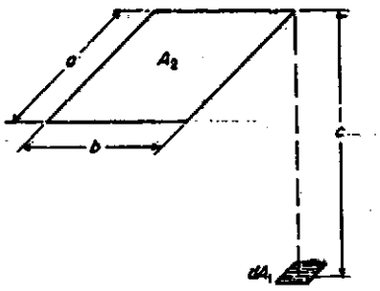

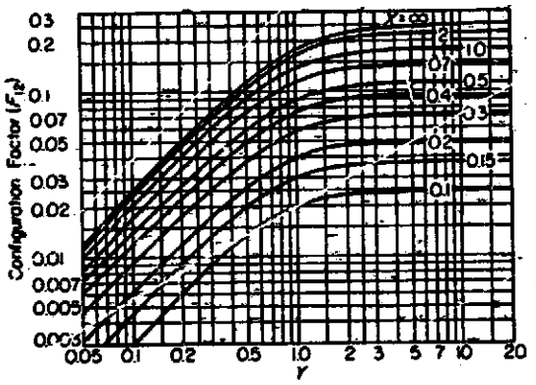

This configuration is a plane point source dA_1 and a plane rectangle A_2 parallel to the plane of dA_1. The normal to dA_1 passes through one corner of A_2. The curves for this configuration are given above where F_{12} is plotted as a function of x and y, with $x = a/c$ and $y = b/c$.

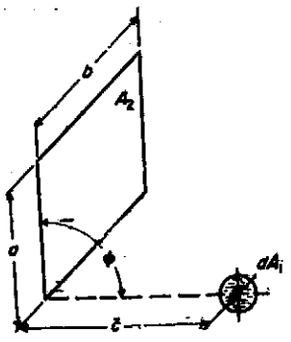

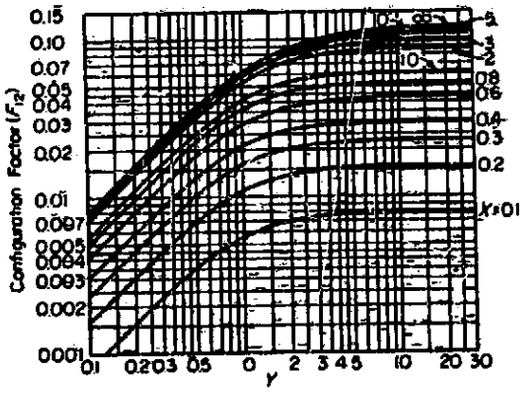

This configuration is a spherical point source dA_1 and a plane rectangle A_2; the point source is located at one corner of a rectangle that has one common side with A_2. The planes of the two rectangles intersect at an angle ϕ. The configuration factor F_{12} is plotted above as a function of x and y, where $x = b/a$ and $y = a/c$.

†Adapted from NACA Report No. TN-4836, by D. C. Hamilton and W. R. Morgan.

Figure 2-22 (Continued)

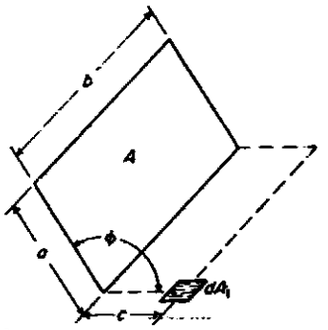

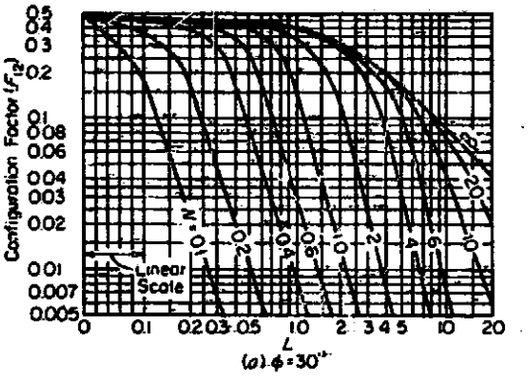

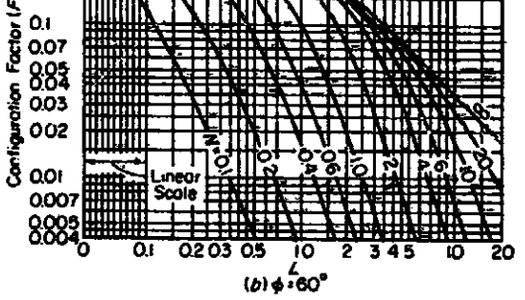

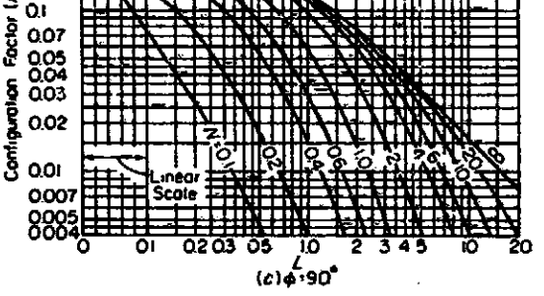

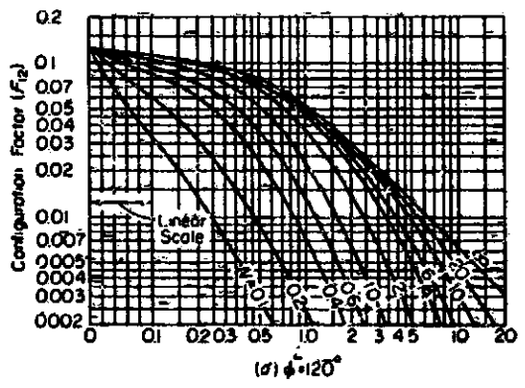

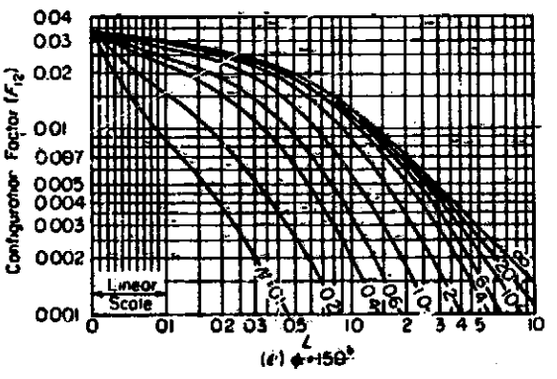

This configuration is a plane point source dA_1 and a plane rectangle A_2, in which the planes of dA_1 and A_2 intersect at an angle $\phi(0° < \phi < 180°)$. The configuration-factor values are given in the curves plotted above for various values of ϕ, N, and L, where $N = a/b$ and $L = c/b$. When $\phi = 0°$, $F_{12} = 0$ for $N < L$ and 0.5 for $N > L$; when $\phi = 180°$, $F_{12} = 0$ for all values of N and L.

Figure 2-22 (Continued)

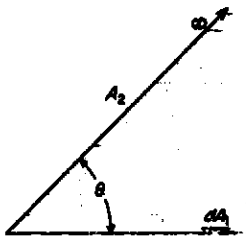

$$F_{12} = \frac{1}{2}(1 + \cos\theta)$$

This configuration is a plane point source dA_1 and any infinite plane A_2, with the planes of dA_1 and A_2 intersecting at an angle θ. The configuration factor values may be calculated from the above equation.

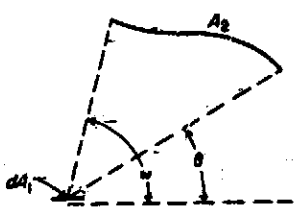

$$F_{12} = \frac{1}{2}(\cos\theta - \cos\omega)$$

This configuration is a plane point source dA_1 and any surface A_2 generated by an infinitely long line, moving parallel to itself and to the plane of dA_1. The configuration-factor values may be computed from the above equation.

Figure 2-22 (Continued)

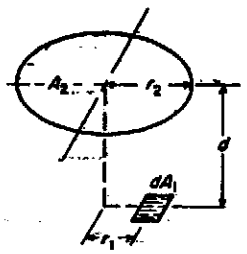

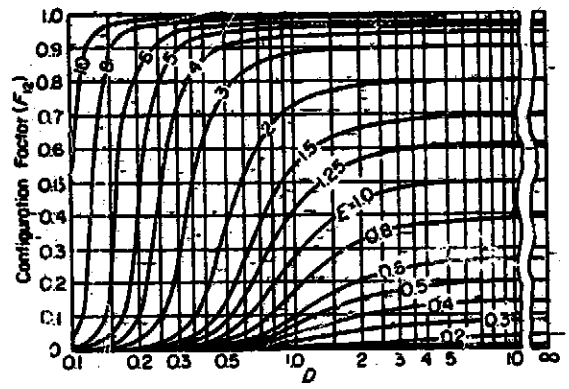

This configuration is a plane point source dA_1 and a plane circular disk A_2. The plane of dA_1 is parallel to the plane of A_2; the point source is located at a distance r_1 from the normal to the center of A_2. The configuration factor F_{12} is plotted above for various values of E and D, where $E = r_2/d$ and $D = d/r_1$.

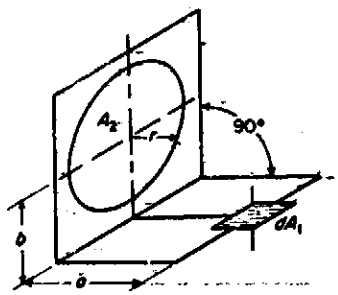

$$F_{12} = \frac{D}{2}\left[\frac{1 + R^2 + D^2}{\sqrt{(1 + R^2 + D^2)^2 - 4R^2}} - 1\right]$$

$$\lim_{R \to 1} F_{12} = \frac{1}{2}\left(\frac{D^2 + 2}{\sqrt{D^2 + 4}} - D\right)$$

This configuration is a plane point source dA_1 and a plane disk A_2; the planes of dA_1 and A_2 intersect at an angle of 90°. The centers of A_2 and dA lie in a plane that is perpendicular to the two planes. The equation above is given in terms of R and D for $R = r/b$ and $D = a/b$.

Figure 2-22 (Continued)

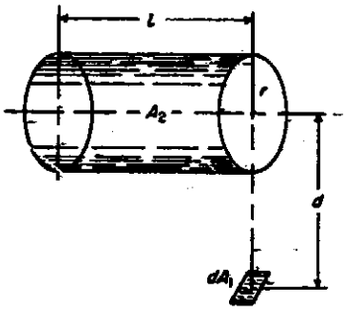

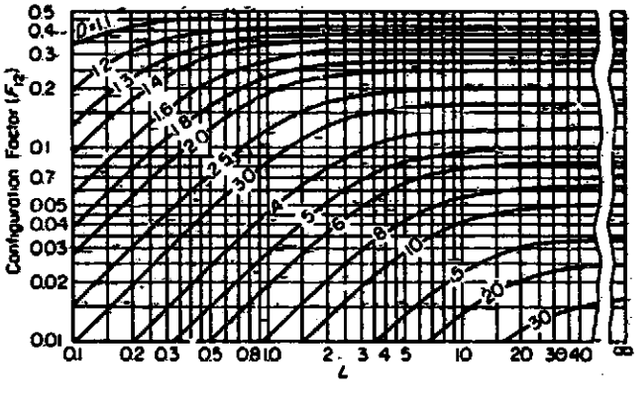

This configuration is a plane point source dA_1 and a right circular cylinder A_2 of length l. The normal to dA_1 passes through the center of one end of the cylinder and is perpendicular to the axis of the cylinder. The configuration factor is plotted above as a function of D and L where $D = d/r$ and $L = l/r$.

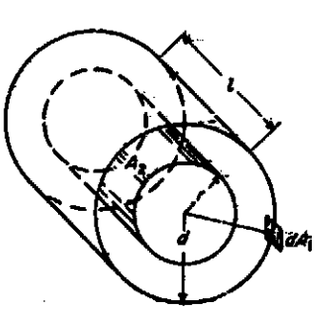

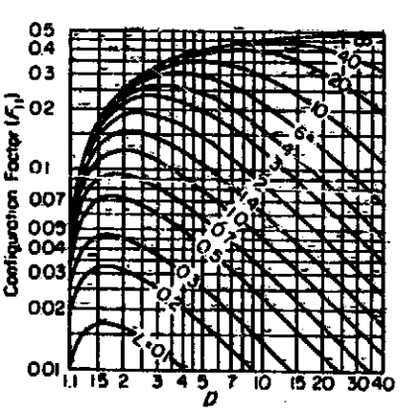

This configuration consists of two concentric cylinders of radius r and d and length l with a point source dA_1 on the inside of the large cylinder at one end. The configuration factor F_{11} is from the point source dA_1 on A_1 to A_1; A_1 does not include the ends of the annulus. The curves for this configuration are given above in terms of D and L, with $D = d/r$ and $L = l/r$.

Figure 2-22 (Concluded)

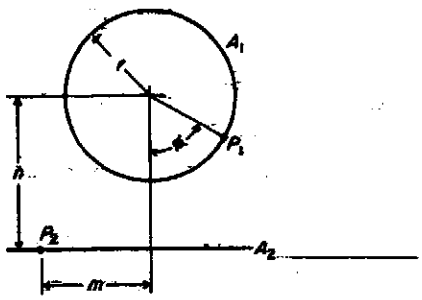

$$F_{P_1-A_2} = \frac{1}{2}(1 + \cos\phi)$$

$$F_{P_2-A_1} = \frac{N}{N^2 - M^2}$$

This configuration consists of an infinitely long cylinder A_1 and an infinite plane A_2, mutually parallel. $M = m/r$ and $N = n/r$.

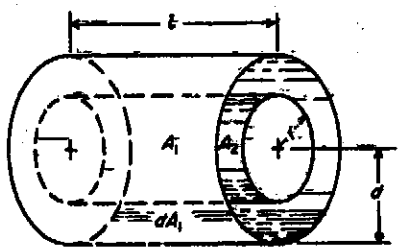

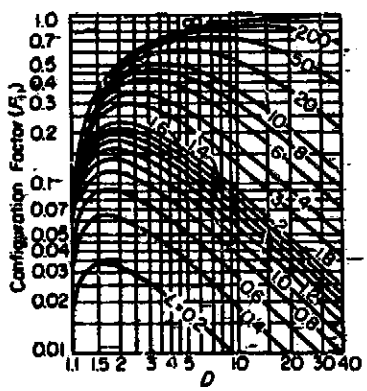

This configuration consists of two concentric cylinders of radius r and d and length L, with element dA_1 on the inside of the large cylinder. The configuration factor F_{11} is from dA_1 to A_1. This factor is plotted above as a function of D and L, with $D = d/r$ and $L = l/r$.

Figure 2-23. Radiant Interchange Configuration Factors†

LINE SOURCES

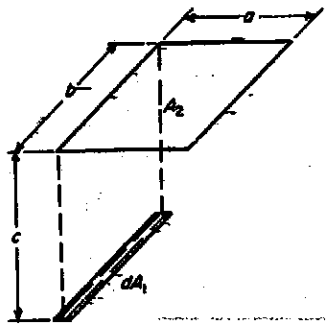

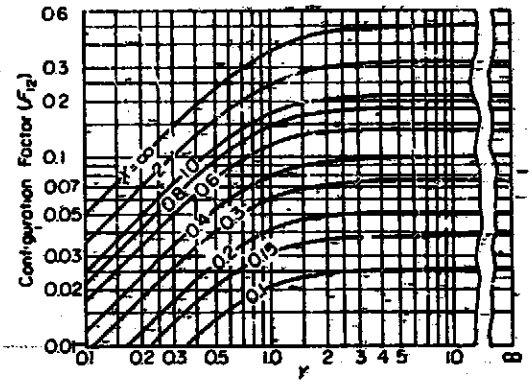

This configuration is a line source dA_1 and a plane rectangle A_2 parallel to the plane of dA_1, with dA_1 opposite one edge of A_2. The plot of F_{12} is a function of x and y, where $x = b/c$ and $y = a/c$.

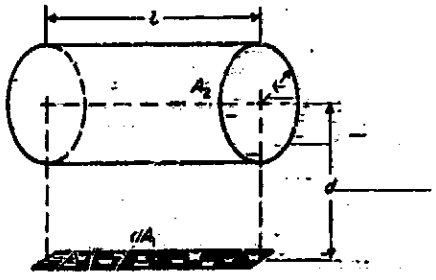

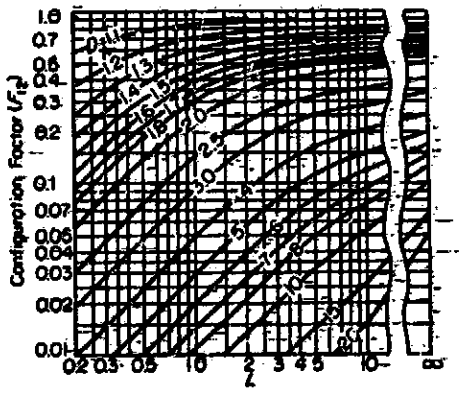

This configuration is a line source dA_1 and a right circular cylinder A_2, both of length l; the normal through each end of the source passes through, and is normal to, the center line of the cylinder at the ends. The configuration factor values are plotted above in terms of the parameters D and L, where $D = d/r$ and $L = l/r$.

†Adapted from NACA Report No. TN-4836, by D. C. Hamilton and W. R. Morgan.

Figure 2-23 (Concluded)

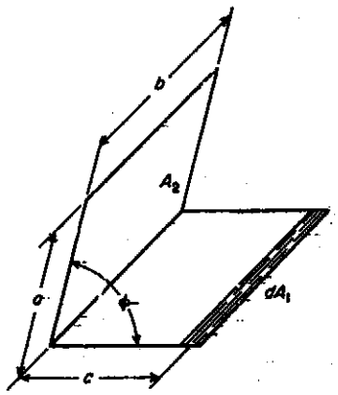

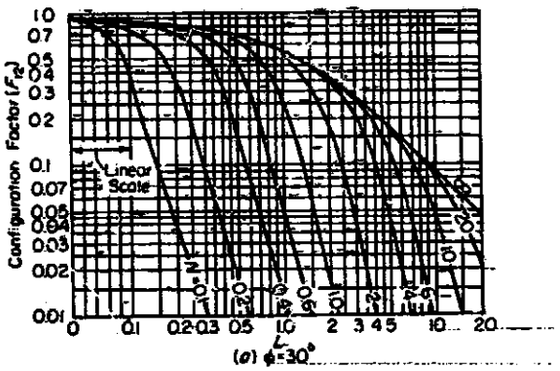

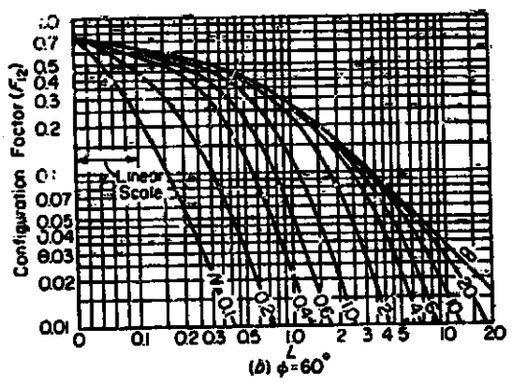

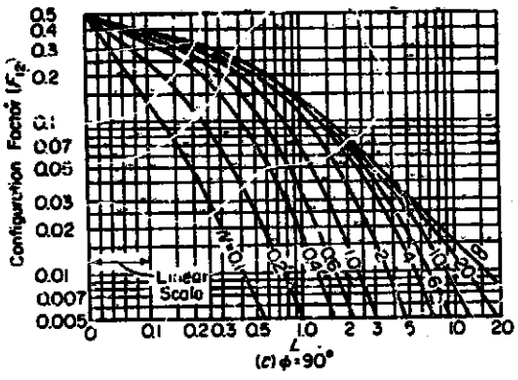

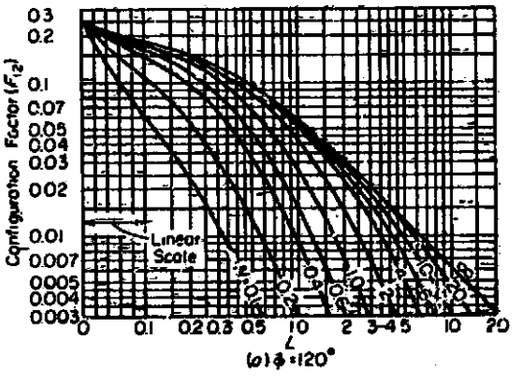

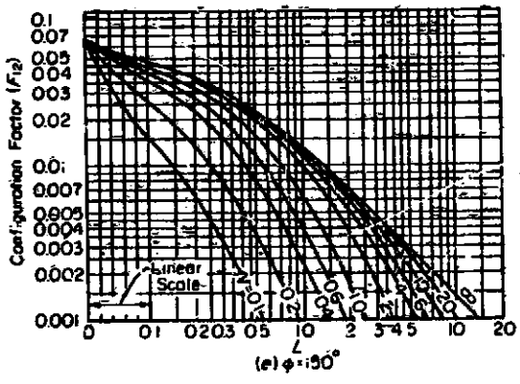

This configuration is a line source dA_1 and a plane rectangle A_2 that intersects the plane of dA_1 at an angle ϕ. The configuration factor is plotted above as a function of N and L for various values of the angle ϕ. $N = a/b$ and $L = c/b$. When $\phi = 0°$, $F_{12} = 0$ for $N < L$ and 1 for $N > L$; when $\phi = 180°$, $F_{12}=0$ for all values of N and L.

Figure 2-24. Radiant - Interchange Configuration Factors†

PLANE SOURCES

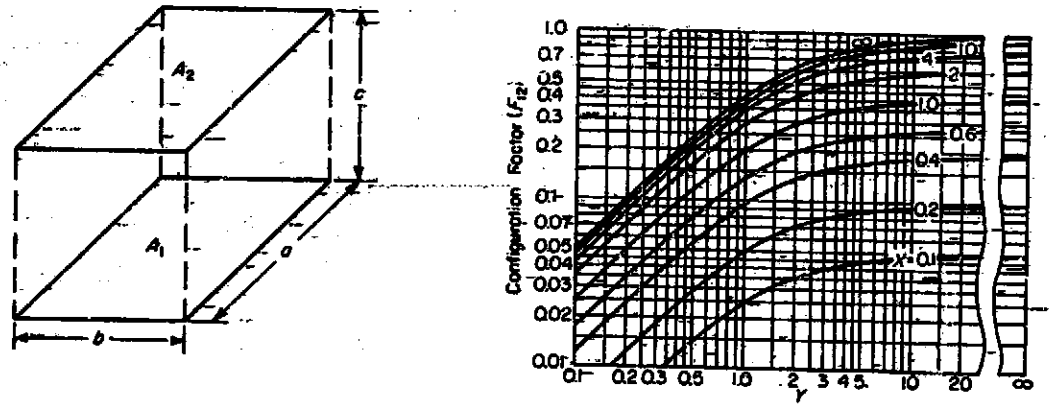

This configuration consists of identical, parallel, directly opposed rectangles A_1 and A_2. The configuration-fact or values are plotted above in terms of the parameters x and y, where $x = b/c$ and $y = a/c$.

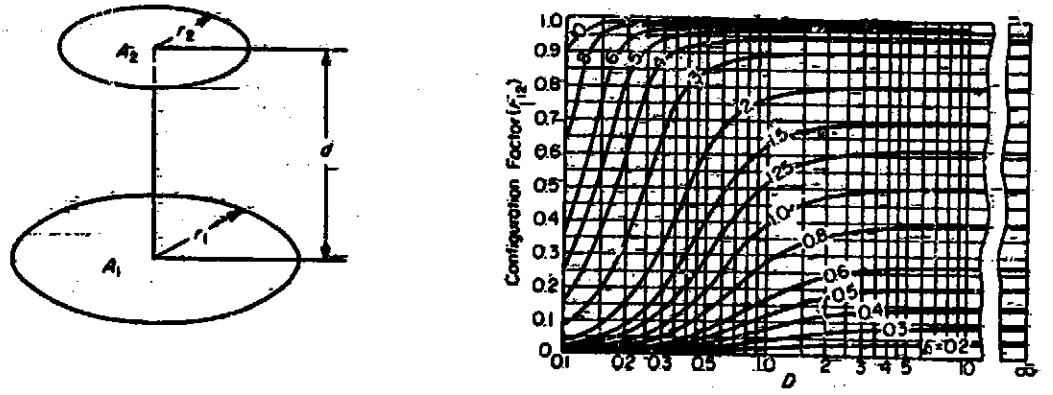

This configuration consists of parallel, directly opposed, plane circular disks. $E = r_2/d$ and $D = d/r_1$.

†Adapted from NACA Report No. TN-4836, by D. C. Hamilton and W. R. Morgan.

Figure 2-24 (Concluded)

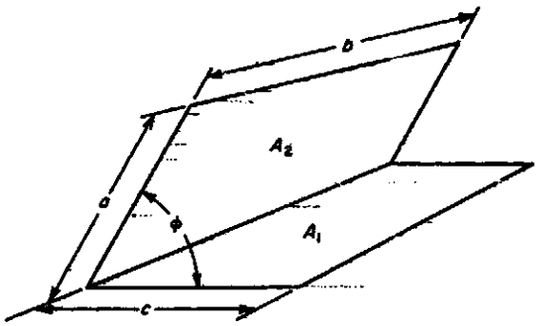

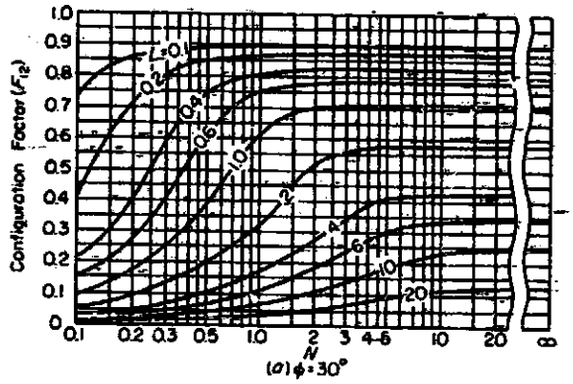

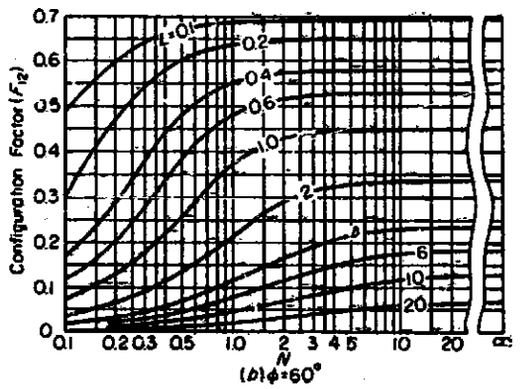

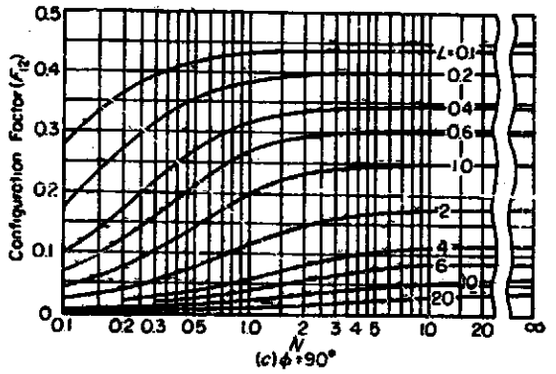

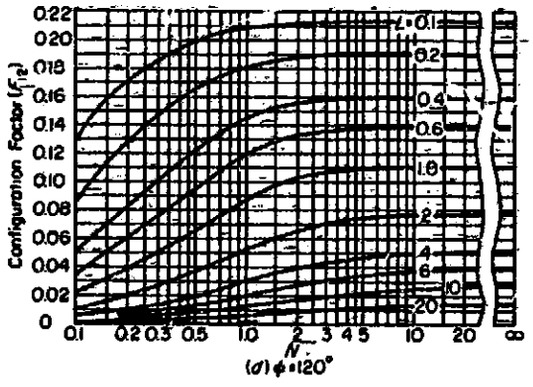

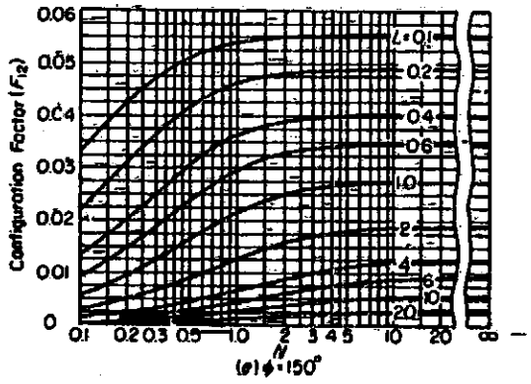

This configuration consists of two rectangles, A_1 and A_2, with one common edge and an included angle between the two planes. The configuration factor is plotted above as a function of N and L for various values of ϕ. $N = a/b$ and $L = c/b$. For $\phi = 90°$, when $\phi = 0°$, $F_{12} = N/L$ for $N < L$ and 1 for $N > L$; when $\phi = 180°$, $F_{12} = 0$ for all values of N and L.

The gray-body shape factor (Script F) $\mathcal{F}_{i-j}$, is the product of the geometric shape factor F_{i-j} and a factor which allows for the departure of the surface from black body conditions. For radiation enclosures, the $\mathcal{F}_{i-j}$ factors are generally evaluated with a computer program. The input for the program being the $A_i F_{i-j}$ values for every surface of the enclosure to every other surface and the emittance and area for each surface. Simplified equations for $\mathcal{F}_{i-j}$ exist for two-component gray enclosures.

Parallel flat plates: $F_{1-2} = F_{2-1} = 1$

$$\mathcal{F}_{1-2} = \frac{1}{\left(\frac{1}{\varepsilon_1} + \frac{1}{\varepsilon_2} - 1\right)}$$

Concentric cylinders of infinite height or concentric spheres:
$F_{1-2} = 1$, $F_{2-1} \neq 0$

$$\mathcal{F}_{1-2} = \frac{1}{\frac{1}{\varepsilon_1} + \frac{A_1}{A_2}\left(\frac{1}{\varepsilon_2} - 1\right)}$$

For "non-enclosed" surfaces an effective emittance, ε_{eff}, between the surfaces may be used to compute the gray-body form factor with the following equation:

$$\mathcal{F}_{i-j} = \varepsilon_{eff\ i}\ F_{i-j}$$

The effective emittance is a function of the emittances of the two surfaces and the configuration factors (E) between them. The error induced with use of ε_{eff} is the result of neglecting secondary reflections from surfaces other than the two for which the effective emittance was determined. By reducing Hottel's method for three flat plate surfaces with emissivities of ε_1, ε_2, and 1, the following equation can be constructed:

$$\varepsilon_{eff} = \frac{\varepsilon_1\ \varepsilon_2}{1 - F_{1-2}\ F_{2-1}\ (1 - \varepsilon_1)\ (1 - \varepsilon_2)}$$

Table 2-4 presents ε_{eff} approximations for various ε_1, ε_2, and $F_{1-2} * F_{2-1}$ values. Intermediate values can be approximated by interpolation.

Table 2-4

FLAT PLATES INSIDE A BLACK ENCLOSURE

EFFECTIVE EMITTANCE FOR F12*F21 = 1.00

EMITTANCE OF SURFACE 1	EMITTANCE OF SURFACE 2											
	1.00	.90	.80	.70	.60	.50	.40	.30	.20	.10	.05	.01
1.00	1.000	.900	.800	.700	.600	.500	.400	.300	.200	.100	.050	.010
.90	.900	.818	.735	.649	.562	.474	.383	.290	.196	.099	.050	.010
.80	.800	.735	.667	.596	.522	.444	.364	.279	.190	.098	.049	.010
.70	.700	.649	.596	.538	.477	.412	.341	.266	.184	.096	.049	.010
.60	.600	.562	.522	.477	.429	.375	.316	.250	.176	.094	.048	.010
.50	.500	.474	.444	.412	.375	.333	.286	.231	.167	.091	.048	.010
.40	.400	.383	.364	.341	.316	.286	.250	.207	.154	.087	.047	.010
.30	.300	.290	.279	.266	.250	.231	.207	.176	.136	.081	.045	.010
.20	.200	.196	.190	.184	.176	.167	.154	.136	.111	.071	.042	.010
.10	.100	.099	.098	.096	.094	.091	.087	.081	.071	.053	.034	.009
.05	.050	.050	.049	.049	.048	.048	.047	.045	.042	.034	.026	.008
.01	.010	.010	.010	.010	.010	.010	.010	.010	.010	.009	.008	.009

FLAT PLATES INSIDE A BLACK ENCLOSURE

EFFECTIVE EMITTANCE FOR F12*F21 = .90

EMITTANCE OF SURFACE 1	EMITTANCE OF SURFACE 2											
	1.00	.90	.80	.70	.60	.50	.40	.30	.20	.10	.05	.01
1.00	1.000	.900	.800	.700	.600	.500	.400	.300	.200	.100	.050	.010
.90	.900	.817	.733	.647	.560	.471	.381	.288	.194	.098	.049	.010
.80	.800	.733	.664	.592	.517	.440	.359	.275	.187	.095	.048	.010
.70	.700	.647	.592	.533	.471	.405	.334	.259	.179	.092	.047	.010
.60	.600	.560	.517	.471	.421	.366	.306	.241	.169	.089	.046	.009
.50	.500	.471	.440	.405	.366	.323	.274	.219	.156	.084	.044	.009
.40	.400	.381	.359	.334	.306	.274	.237	.193	.141	.078	.041	.009
.30	.300	.288	.275	.259	.241	.219	.193	.161	.121	.069	.037	.008
.20	.200	.194	.187	.179	.169	.156	.141	.121	.094	.057	.032	.007
.10	.100	.098	.095	.092	.089	.084	.078	.069	.057	.037	.022	.005
.05	.050	.049	.048	.047	.046	.044	.041	.037	.032	.022	.013	.003
.01	.010	.010	.010	.010	.009	.009	.009	.008	.007	.005	.003	.001

Table 2-4 (Continued)

FLAT PLATES INSIDE A BLACK ENCLOSURE

EFFECTIVE EMITTANCE FOR F12*F21 = .80

EMITTANCE OF SURFACE 2

EMITTANCE OF SURFACE 1	1.00	.90	.80	.70	.60	.50	.40	.30	.20	.10	.05	.01
1.00	1.000	.900	.800	.700	.600	.500	.400	.300	.200	.100	.050	.010
.90	.900	.817	.732	.645	.558	.469	.378	.286	.192	.097	.049	.010
.80	.800	.732	.661	.588	.513	.435	.354	.270	.183	.093	.047	.010
.70	.700	.645	.588	.528	.465	.398	.327	.252	.173	.089	.045	.009
.60	.600	.558	.513	.465	.413	.357	.297	.232	.161	.084	.043	.009
.50	.500	.469	.435	.398	.357	.312	.263	.208	.147	.078	.040	.008
.40	.400	.378	.354	.327	.297	.263	.225	.181	.130	.070	.037	.008
.30	.300	.286	.270	.252	.232	.208	.181	.148	.109	.060	.032	.007
.20	.200	.192	.183	.173	.161	.147	.130	.109	.082	.047	.026	.005
.10	.100	.097	.093	.089	.084	.078	.070	.060	.047	.028	.016	.003
.05	.050	.049	.047	.045	.043	.040	.037	.032	.026	.016	.009	.002
.01	.010	.010	.010	.009	.009	.008	.008	.007	.005	.003	.002	.000

FLAT PLATES INSIDE A BLACK ENCLOSURE

EFFECTIVE EMITTANCE FOR F12*F21 = .70

EMITTANCE OF SURFACE 2

EMITTANCE OF SURFACE 1	1.00	.90	.80	.70	.60	.50	.40	.30	.20	.10	.05	.01
1.00	1.000	.900	.800	.700	.600	.500	.400	.300	.200	.100	.050	.010
.90	.900	.816	.730	.644	.556	.466	.376	.284	.191	.096	.048	.010
.80	.800	.730	.658	.585	.508	.430	.349	.266	.180	.092	.046	.009
.70	.700	.644	.585	.523	.459	.391	.320	.246	.168	.086	.044	.009
.60	.600	.556	.508	.459	.405	.349	.288	.224	.155	.080	.041	.008
.50	.500	.466	.430	.391	.349	.303	.253	.199	.139	.073	.037	.008
.40	.400	.376	.349	.320	.288	.253	.214	.170	.120	.064	.033	.007
.30	.300	.284	.266	.246	.224	.199	.170	.137	.099	.054	.028	.006
.20	.200	.191	.180	.168	.155	.139	.120	.099	.072	.040	.021	.004
.10	.100	.096	.092	.086	.080	.073	.064	.054	.040	.023	.012	.003
.05	.050	.048	.046	.044	.041	.037	.033	.028	.021	.012	.007	.001
.01	.010	.010	.009	.009	.008	.008	.007	.006	.004	.003	.001	.000

Table 2-4 (Continued)

FLAT PLATES INSIDE A BLACK ENCLOSURE

EFFECTIVE EMITTANCE FOR F12=F21 = .60

EMITTANCE OF SURFACE 2

EMITTANCE OF SURFACE 1	1.00	.90	.80	.70	.60	.50	.40	.30	.20	.10	.05	.01
1.00	1.000	.900	.800	.700	.600	.500	.400	.300	.200	.100	.050	.010
.90	.900	.815	.729	.642	.553	.464	.373	.282	.189	.095	.048	.010
.80	.800	.729	.656	.581	.504	.426	.345	.262	.177	.090	.045	.009
.70	.700	.642	.581	.518	.453	.385	.314	.240	.164	.084	.042	.009
.60	.600	.553	.504	.453	.398	.341	.280	.216	.149	.077	.039	.008
.50	.500	.464	.426	.385	.341	.294	.244	.190	.132	.068	.035	.007
.40	.400	.373	.345	.314	.280	.244	.204	.160	.112	.059	.030	.006
.30	.300	.282	.26	.240	.216	.190	.160	.127	.090	.048	.025	.005
.20	.200	.189	.177	.164	.149	.132	.112	.090	.065	.035	.018	.004
.10	.100	.095	.090	.084	.077	.068	.059	.048	.035	.019	.010	.002
.05	.050	.048	.045	.042	.039	.035	.030	.025	.018	.010	.005	.001
.01	.010	.010	.009	.009	.008	.007	.006	.005	.004	.002	.001	.000

FLAT PLATES INSIDE A BLACK ENCLOSURE

EFFECTIVE EMITTANCE FOR F12=F21 = .50

EMITTANCE OF SURFACE 2

EMITTANCE OF SURFACE 1	1.00	.90	.80	.70	.60	.50	.40	.30	.20	.10	.05	.01
1.00	1.000	.900	.800	.700	.600	.500	.400	.300	.200	.100	.050	.010
.90	.900	.814	.729	.640	.551	.462	.371	.280	.187	.094	.047	.009
.80	.800	.729	.655	.577	.500	.421	.340	.258	.174	.088	.044	.009
.70	.700	.640	.577	.513	.447	.378	.305	.232	.159	.081	.041	.008
.60	.600	.551	.500	.447	.391	.333	.273	.209	.143	.073	.037	.007
.50	.500	.462	.421	.378	.333	.286	.235	.182	.125	.065	.033	.007
.40	.400	.371	.340	.305	.273	.235	.195	.152	.105	.055	.028	.006
.30	.300	.280	.258	.232	.209	.182	.152	.119	.083	.044	.022	.005
.20	.200	.187	.174	.159	.143	.125	.105	.083	.059	.031	.016	.003
.10	.100	.094	.088	.081	.073	.065	.055	.044	.031	.017	.009	.002
.05	.050	.047	.044	.041	.037	.033	.028	.022	.016	.009	.005	.001
.01	.010	.009	.009	.008	.007	.007	.006	.005	.003	.002	.001	.000

Table 2-4 (Continued)

FLAT PLATES INSIDE A BLACK ENCLOSURE

EFFECTIVE EMITTANCE FOR F12*F21 = .40

EMITTANCE OF SURFACE 2

EMITTANCE OF SURFACE 1	1.00	.90	.80	.70	.60	.50	.40	.30	.20	.10	.05	.01
1.00	1.000	.900	.800	.700	.600	.500	.400	.300	.200	.100	.050	.010
.90	.900	.813	.726	.638	.549	.459	.369	.278	.186	.093	.047	.009
.80	.800	.726	.650	.574	.496	.417	.336	.254	.171	.086	.043	.009
.70	.700	.638	.574	.508	.441	.372	.302	.229	.155	.078	.040	.008
.60	.600	.549	.496	.441	.385	.326	.265	.203	.138	.070	.035	.007
.50	.500	.459	.417	.372	.326	.278	.227	.174	.119	.061	.031	.006
.40	.400	.369	.336	.302	.265	.227	.187	.144	.099	.051	.026	.005
.30	.300	.278	.254	.229	.203	.174	.144	.112	.077	.040	.020	.004
.20	.200	.186	.171	.155	.138	.119	.099	.077	.054	.028	.014	.003
.10	.100	.093	.086	.078	.070	.061	.051	.040	.028	.015	.008	.002
.05	.050	.047	.043	.040	.035	.031	.026	.020	.014	.008	.004	.001
.01	.010	.009	.009	.008	.007	.006	.005	.004	.003	.002	.001	.000

FLAT PLATES INSIDE A BLACK ENCLOSURE

EFFECTIVE EMITTANCE FOR F12*F21 = .30

EMITTANCE OF SURFACE 2

EMITTANCE OF SURFACE 1	1.00	.90	.80	.70	.60	.50	.40	.30	.20	.10	.05	.01
1.00	1.000	.900	.800	.700	.600	.500	.400	.300	.200	.100	.050	.010
.90	.900	.812	.724	.636	.547	.457	.367	.276	.184	.092	.046	.009
.80	.800	.724	.648	.570	.492	.412	.332	.251	.168	.085	.042	.009
.70	.700	.636	.570	.504	.436	.366	.296	.224	.151	.078	.038	.008
.60	.600	.547	.492	.436	.378	.319	.259	.197	.133	.067	.034	.007
.50	.500	.457	.412	.366	.319	.270	.220	.168	.114	.058	.029	.006
.40	.400	.367	.332	.296	.259	.220	.179	.137	.093	.048	.024	.005
.30	.300	.276	.251	.224	.197	.168	.137	.106	.072	.037	.019	.004
.20	.200	.184	.168	.151	.133	.114	.093	.072	.050	.026	.013	.003
.10	.100	.092	.085	.076	.067	.058	.048	.037	.026	.013	.007	.001
.05	.050	.046	.042	.038	.034	.029	.024	.019	.013	.007	.003	.001
.01	.010	.009	.009	.008	.007	.006	.005	.004	.003	.001	.001	.000

Table 2-4 (Continued)

FLAT PLATES INSIDE A BLACK ENCLOSURE

EFFECTIVE EMITTANCE FOR F12*F21 = .20

EMITTANCE OF SURFACE 1	EMITTANCE OF SURFACE 2											
	1.00	.90	.80	.70	.60	.50	.40	.30	.20	.10	.05	.01
1.00	1.000	.900	.800	.700	.600	.500	.400	.300	.200	.100	.050	.010
.90	.900	.812	.723	.634	.544	.455	.364	.274	.183	.092	.046	.009
.80	.800	.723	.645	.567	.488	.408	.328	.247	.165	.083	.042	.008
.70	.700	.634	.567	.498	.430	.361	.290	.219	.147	.074	.037	.007
.60	.600	.544	.488	.430	.372	.312	.252	.191	.128	.065	.032	.007
.50	.500	.455	.408	.361	.312	.263	.213	.161	.109	.055	.028	.006
.40	.400	.364	.328	.290	.252	.213	.172	.131	.088	.045	.023	.005
.30	.300	.274	.247	.219	.191	.161	.131	.100	.068	.034	.017	.003
.20	.200	.183	.165	.147	.128	.109	.088	.068	.046	.023	.012	.002
.10	.100	.092	.083	.074	.065	.055	.045	.034	.023	.012	.006	.001
.05	.050	.046	.042	.037	.032	.028	.023	.017	.012	.006	.003	.001
.01	.010	.009	.008	.007	.007	.006	.005	.003	.002	.001	.001	.000

FLAT PLATES INSIDE A BLACK ENCLOSURE

EFFECTIVE EMITTANCE FOR F12*F21 = .10

EMITTANCE OF SURFACE 1	EMITTANCE OF SURFACE 2											
	1.00	.90	.80	.70	.60	.50	.40	.30	.20	.10	.05	.01
1.00	1.000	.900	.800	.700	.600	.500	.400	.300	.200	.100	.050	.010
.90	.900	.811	.721	.632	.542	.452	.362	.272	.181	.091	.045	.009
.80	.800	.721	.642	.563	.484	.404	.324	.243	.163	.081	.041	.008
.70	.700	.632	.563	.494	.425	.355	.285	.215	.143	.072	.036	.007
.60	.600	.542	.484	.425	.366	.306	.246	.185	.124	.062	.031	.006
.50	.500	.452	.404	.355	.306	.256	.206	.155	.104	.052	.026	.005
.40	.400	.362	.324	.285	.246	.206	.166	.125	.084	.042	.021	.004
.30	.300	.272	.243	.215	.185	.155	.125	.095	.064	.032	.016	.003
.20	.200	.181	.163	.143	.124	.104	.084	.064	.043	.022	.011	.002
.10	.100	.091	.081	.072	.062	.052	.042	.032	.022	.011	.005	.001
.05	.050	.045	.041	.036	.031	.026	.021	.016	.011	.005	.003	.001
.01	.010	.009	.008	.007	.006	.005	.004	.003	.002	.001	.001	.000

Table 2-4 (Concluded)

FLAT PLATES INSIDE A BLACK ENCLOSURE

EFFECTIVE EMITTANCE FOR F12*F21 = .05

EMITTANCE OF SURFACE 1	EMITTANCE OF SURFACE 2											
	1.00	.90	.80	.70	.60	.50	.40	.30	.20	.10	.05	.01
1.00	1.000	.900	.800	.700	.600	.500	.400	.300	.200	.100	.050	.010
.90	.900	.810	.721	.631	.541	.451	.361	.271	.181	.090	.045	.009
.80	.800	.721	.641	.562	.482	.402	.322	.242	.161	.081	.040	.008
.70	.700	.631	.562	.492	.423	.353	.283	.212	.142	.071	.036	.007
.60	.600	.541	.482	.423	.363	.303	.243	.183	.122	.061	.031	.006
.50	.500	.451	.402	.353	.303	.253	.203	.153	.102	.051	.026	.005
.40	.400	.361	.322	.283	.243	.203	.163	.123	.082	.041	.021	.004
.30	.300	.271	.242	.212	.183	.153	.123	.092	.062	.031	.016	.003
.20	.200	.181	.161	.142	.122	.102	.082	.062	.041	.021	.010	.002
.10	.100	.090	.081	.071	.061	.051	.041	.031	.021	.010	.005	.001
.05	.050	.045	.040	.036	.031	.026	.021	.016	.010	.005	.003	.001
.01	.010	.009	.008	.007	.006	.005	.004	.003	.002	.001	.001	.000

FLAT PLATES INSIDE A BLACK ENCLOSURE

EFFECTIVE EMITTANCE FOR F12*F21 = .01

EMITTANCE OF SURFACE 1	EMITTANCE OF SURFACE 2											
	1.00	.90	.80	.70	.60	.50	.40	.30	.20	.10	.05	.01
1.00	1.000	.900	.800	.700	.600	.500	.400	.300	.200	.100	.050	.010
.90	.900	.810	.720	.630	.540	.450	.360	.270	.180	.090	.045	.009
.80	.800	.720	.640	.560	.480	.400	.320	.240	.160	.080	.040	.008
.70	.700	.630	.560	.490	.421	.351	.281	.210	.140	.070	.035	.007
.60	.600	.540	.480	.421	.361	.301	.241	.181	.120	.060	.030	.006
.50	.500	.450	.400	.351	.301	.251	.201	.151	.100	.050	.025	.005
.40	.400	.360	.320	.281	.241	.201	.161	.121	.080	.040	.020	.004
.30	.300	.270	.240	.210	.181	.151	.121	.090	.060	.030	.015	.003
.20	.200	.180	.160	.140	.120	.100	.080	.060	.040	.020	.010	.002
.10	.100	.090	.080	.070	.060	.050	.040	.030	.020	.010	.005	.001
.05	.050	.045	.040	.035	.030	.025	.020	.015	.010	.005	.003	.001
.01	.010	.009	.008	.007	.006	.005	.004	.003	.002	.001	.001	.000

2.2.2.6 Computational Methods - Mass Flow Conductors

The use of a mass flow conductor in a thermal network is a convenient method of accounting for the transfer of energy from one point to another due to the actual movement (flow) of a fluid from one point to another. Mass flow conductors are computed from the equation:

$$G = \dot{W} C_p$$

where:

$\dot{W}$ = the mass flow rate of the fluid - LB/HR

C_p = fluid specific heat - BTU/LB-°F

The mass flow rate ($\dot{W}$) is related to the fluid velocity by the expression:

$$\dot{W} = \rho A U$$

where:

A = the cross sectional area through which the fluid flows - FT^2

U = the fluid velocity - FT/HR

ρ = the fluid density - LB/FT^3

The thermophysical properties C_p and ρ should be evaluated at the bulk temperature of the fluid.

The mass flow conductor which is in addition to any other mode of heat transfer simply accounts for the internal energy term of a mass moving from one location to another.

2.2.3 Energy Sources or Sinks

2.2.3.1 Concepts

Energy sources or sinks, Q, are modeling elements which allow the impression of positive or negative heating rates on the nodes of a thermal network independent of conductor paths to the node.

2.2.3.2 Types of Heat Sources or Sinks

Common engineering applications of heat sources in thermal models are:

- Solar and Planetary Heating
- Aerodynamic Heating
- Avionic Coldplate Heat Loads
- Change of State Latent Energy
- Thermal Control Heaters

Common application for heat sinks are:

- Change of State Latent Energy
- Radiator Heat Rejection
- Aerodynamic Cooling

2.2.3.3 Computational Considerations - Sources or Sinks

Heating rates may be impressed on diffusion (finite capacitance) or arithmetic (zero capacitance) nodes. Most thermal analyzers provide a separate entry block for entering heating or cooling rates. For example, the SINDA computer program uses the SOURCE DATA BLOCK for such entries. In the usual case, heating rates are not considered when computing the time steps for transient analysis, and large heating rates on low capacitance nodes may create instability in the network solution. Also the impression of large heat sources on arithmetic nodes with radiation (nonlinear) conductors attached often causes large erroneous temperature oscillations in the arithmetic and adjoining nodes. Both of these difficulties can be avoided with the use of the program control constants incorporated in most thermal network analyzers. These control constants are the time step multiplication factor and the maximum temperature change allowed.

2.3 Network Solution

An area which is of utmost concern to the engineer is an explanation of the system of equations which are solved in a typical thermal problem. At this point it must be completely understood that the physical system is reduced to a lumped (nodalized) system and that the choice of the nodalization has a far greater bearing on the problem than the particular numerical solution technique and assumptions that are usually employed in the problem solution. Each numerical solution method is bounded by accuracy constraints dictated by the particular set of assumptions associated with the particular problem undergoing solution.

The basic transient heat transfer equation applied to linear conduction problems is:

$$\frac{\partial T}{\partial t} = \alpha \nabla^2 T \quad \nabla^2 = \frac{\partial^2}{\partial x^2} + \frac{\partial^2}{\partial y^2} + \frac{\partial^2}{\partial z^2} \tag{1}$$

The solution techniques most commonly applied stem from a reduction of Equation (1). It can be easily seen that any nonlinear terms such as radiation must be linearized by some method if the above equation is to be used.

For example the radiation term $G(T_i^4 - T_j^4)$ can be linearized by

$$G\gamma(T_i - T_j) = G(T_i^4 - T_j^4) \tag{2}$$

where γ is the linearization factor. The calculation of γ and the linearization of the G's is performed automatically by thermal network analyzers and will be explained in more detail in the forward differencing section.

The process of nodalization reduces the volumetric dimensions and properties so that equation (1) can be cast in the following form:

$$\frac{dT_i}{dt} = \sum_j \frac{G_{ij}(T_j - T_i)}{C_i} \tag{3}$$

Each term of the summation, $G_{ij}(T_j-T_i)$, represents the heat rate, $\dot{Q}$, following into node - i from node - j. Integrating equation (3) yields:

$$T_i(t_{new}) = T_i(t_{old}) + \frac{1}{C_i}\int_{t_{old}}^{t_{new}} \sum_j G_{ij}(T_j-T_i)dt \qquad (4)$$

To actually perform the integration indicated in equation (4) on a computer it would be most convenient if the integrand was not a function of time:

$$\text{i.e.:} \quad \sum_j G_{ij}(T_j-T_i) \Big|_{t_{old}}^{t_{new}} = \bar{Q}_i = \text{constant} \qquad (5)$$

If this was the case, then the second term in equation (4) would reduce to:

$$\frac{1}{C_i}\int_{t_{old}}^{t_{new}} \sum_j G_{ij}(T_j-T_i)\,dt = \frac{\dot{Q}_i\,(t_{new} - t_{old})}{C_i} = \frac{\dot{Q}_i}{C_i}\,\Delta t \qquad (6)$$

and equation (4) could be cast in the simple form of:

$$T_i(t+\Delta t) = T_i(t) + \frac{\dot{Q}_i}{C_i}\,\Delta t \qquad (7)$$

Equation (7) represents the basic finite differencing formulation of the transient heat transfer equation. All finite differencing methods, be they forward, backward, central, explicit or implicit, perform the calculation indicated in equation (7). The only difference among the various formulations lies in the assumption used to evaluate the Q_i term per equation (6). The significance of this assumption as it relates to the various finite differencing formulations will be discussed in following seetions.

2.3.1 Steady State

A thermal system has reached the steady state when the net heat flow rate to each diffusion and arithmetic node is zero. From equation (3), this yields:

$$\sum_j G_{ij}(T_j - T_i) = 0 \tag{8}$$

Rearranging the terms in equation (8) yields

$$T_i = \frac{\sum_j G_{ij} T_j}{\sum_j G_{ij}} \tag{9}$$

The subscripts in equation (9) obscure the elegance of the steady state solution, which can also be expressed as:

$$\underline{T} = [G]\,\underline{T} \tag{10}$$

Equation (10) clearly reveals that finding the steady state temperature vector simply amounts to finding the eigenvector of [G] for an eigenvalue of 1. The only problem is that, for a network with more than a few (say 20) nodes, the calculation of the eigenvector using an explicit algorithm, such as Gaussian Elimination, would take a prohibitive amount of time. This, in addition to the fact that most of the elements of [G] are zero, suggests that an iterative technique such as expressed in equation (11) would result in a huge reduction in required computer time.

$$\underline{T}^{i+1} = [G]\,T^{i} \tag{11}$$

When it is also realized that equation (10) is only valid when the G matrix is absolutely constant with respect to temperature, it becomes clear that equation (11) is the only solution technique that is universally usable. Using this technique, it is simple matter to update the G matrix (evaluate temperature varying G's and linearize radiation G's) based on the new guess

temperature vector $\underline{T}^{i+1}$ before proceeding to the next iteration. In addition, equation (11) does not require that the $\underline{T}^{i+1}$ and $\underline{T}^{i}$ vectors be the same length, so that the $\underline{T}^{i}$ vector can be extended to include a vector of temperatures which represent the boundary conditions placed on the network.

Two criteria for terminating the iterative process are generally provided. The first is simply a fixed number, N, which represents the maximum number of iterations to be performed. The second is a convergence or, as it is more commonly called, a relaxation criterion, δ, which is defined as:

$$\max_j T_j^{i+1} - T_j^{i} \leq \delta \qquad (12)$$

In other words, calculations cease when no "significant" improvement from one iteration to the next is noted (where "significant" is defined in terms of δ).

Strong oscillation in the temperature vector is often noted when analyzing a network which is dominated by radiation effects. To hasten (and in some cases, to enable) the convergence of the solution, a damping factor, ζ, is often applied to equation (11) to yield the more versatile solution technique expressed in equation (13).

$$\underline{T}^{i+1} = \zeta [G] \underline{T}^{i} + (1-\zeta) \underline{T}^{i} \qquad (0 < \zeta \leq 1) \qquad (13)$$

To summarize, the fully general finite differencing technique for steady state analysis is an iterative algorithm requiring three parameters, N, δ, and ζ, for the control of convergence. It might be noted here that arithmetic nodes always receive a steady state solution technique even when they appear in a network which is undergoing a transient analysis.

2.3.2 Transient Analysis

2.3.2.1 Forward Differencing

Forward differencing derives its name from the fact that all temperatures are extrapolated forward in time, t, for the purpose of evaluating the expression in equation (5). This point is illustrated in Figure 2-25.

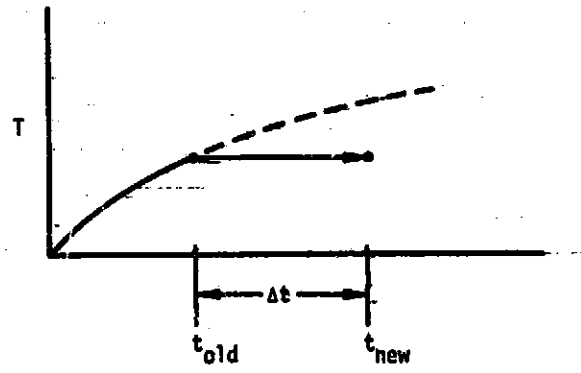

Figure 2-25. Forward Extrapolation Used in Forward Differencing

Combining equations (5) and (7) under the above assumption yields the basic forward differencing equation:

$$T_i(t+\Delta t) = T_i(t) + \frac{\Delta t}{C_i} \sum_j G_{ij}(T_j(t) - T_i(t)) \qquad (14)$$

As might be expected, the temperatures at time t are used to evaluate any temperature varying or radiation conductors. That is, for example, the linearization factor, γ, is computed as:

$$\gamma = (T_j^2(t) + T_i^2(t))\,(T_j(t) + T_i(t)) \qquad (15)$$

The basic forward extrapolation assumption has two consequences: (a) the resulting solution equation is explicit, and (b) the solution can be unstable. When it is stated that an equation is explicit, it means that all of the unknowns are on the left hand side and all of the known quantities are on the right hand side. Since all of the temperatures at time t are known, equation (14) defines the temperatures at time

$t + \Delta t$, explicitly. Instability results from the fact that equation (14) is, so to speak, "open-ended". By choosing a sufficiently large Δt, the new temperatures can be made unreasonable. It has been shown (reference 3), however, that if Δt is restricted to be less than the stability factor, τ, defined in equation (16), then the solution normally will be stable.

$$\min_i \frac{C_i}{\sum_j G_{ij}} = \tau = \text{CSGMIN} \qquad (16)$$

This τ, commonly called "the CSGMIN," is the smallest time constant in the thermal network. The "CSGMIN" does not include boundary effects. Sharp gradients coupled with high magnitude heating rates could possibly cause instability.

It is clear, then, that forward differencing represents a two-edged sword. On the one hand, the solution equation is explicit, which means that the volume of computations for each Δt step will be a minimum. But on the other hand, the size of the time step is limited to the smallest time constant in the entire network. However, additional advantages accrue from both of these conditions. First, the user need not specify any convergence criteria such as were required by the steady state technique, and second, for normal cases the user need not specify the time step, Δt, since this can be conveniently computed by the computer using a simple algorithm such as given in equation (17).

$$\Delta t = 95\% \ \tau \qquad (17)$$

Another moderating point to be considered is that the maximum Δt used for a transient analysis is often not restricted by the network, but rather by the frequency spectrum of the boundary conditions. In gross terms, one cannot use a Δt of one hour to analyze a network subjected to a boundary condition which varies at the rate of 50 cycles per hour. In finer terms, Shannon's Sampling Theorem (reference 4) dictates that:

$$\omega_s > 2\omega_c \tag{18}$$

or:

$$\max \Delta t < \frac{1}{2\omega_c} \tag{19}$$

where ω_c is the highest frequency component in the driving signal. Of course, the limit expressed in equation (19) is theoretical in that it assumes that the system is a perfect low-pass filter. This is true, in practice, only at nodal points rather far away from the boundary. Hence, analyses of the temperature response near rapidly varying boundaries will require a Δt much smaller than the maximum expressed in equation (19).

It is no accident, then, that forward differencing formulations enjoy the widest and most frequent use in engineering practice. Other formulations have practical value only when the choice of Δt is not restricted by boundary conditions.

2.3.2.2 Backward Differencing

Backward differencing takes its name from the fact that all temperatures at time tnew are extrapolated backward in time in order to evaluate the $\dot{Q}$ terms per equation 1-15. This point is illustrated in Figure 2-26.

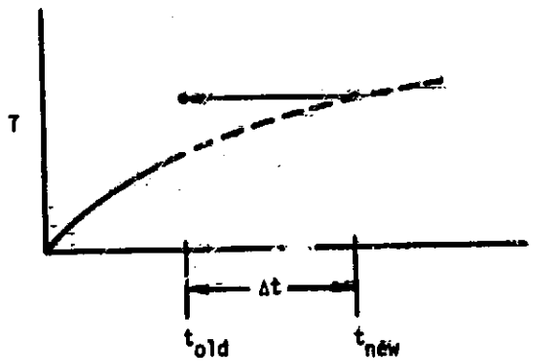

Figure 2-26. Backward Extrapolation Used in Backward Differencing

Using this assumption to combine equations (5) and (7), and stating the result in matrix form yields:

$$\underline{T}\,(t+\Delta t) = \underline{T}\,(t) + \Delta t\,[G/C]\,\underline{T}\,(t+\Delta t) \qquad (20)$$

The solution to equation (2) obviously requires that a matrix inversion be performed, but it also requires, strictly, that the G/C matrix be temperature invariant. (Otherwise, the basic assumption would require that [G/C] be evaluated for $\underline{T} = \underline{T}(t+\Delta t)$, and, of course, these temperatures are not yet known.) In practice, then, equation (20) is reworked into a form which lends itself to iterative calculations.

$$T_i^{\ell+1}\,(t+\Delta) = \frac{\frac{C_i}{\Delta t}\,T_i(t) + \sum_j G_{ij}T_j^{\ell}(t+\Delta t)}{\frac{C_i}{\Delta t} + \sum_j G_{ij}} \qquad (21)$$

Since $T(t+\Delta t)$ appears on both sides of the equation, this formulation is termed an <u>implicit</u> solution technique.

It will be noted that when Δt approaches infinity, equation (21) reduces to the steady state equation discussed in Section 2.3.1. Hence, it can be deduced (and it has been proven in reference 3) that backward differencing is stable for any Δt. In addition, backward differencing is subject to the same set of iteration termination criteria, N and δ, as were applied to the steady state solution. Stability for large Δt, however, does not preclude the possibility of an oscillating solution, so a damping factor, ζ, is also provided to ensure the eventual convergence to the solution.

The great advantage of backward differencing lies in the effective selection of Δt. During periods of rapidly varying boundary conditions, Δt may be reduced to as small a value as desired, and then, during periods of slowly drifting boundary conditions, it can be enlarged to a compatible

value, without regard for the minimum time constant, τ, of the network. It also happens that when a large Δt is appropriate, the number of iterations necessary to satisfy the relaxation criterion, δ, is relatively small. On the other hand, when Δt is compressed to less than the CSGMIN (τ), the number of iterations per time step will still be large when compared to forward differencing.

2.3.3 Summary of Other Techniques

Numerous other approaches to formulating finite differencing solutions are available (reference 5). However, all of these generally amount to modifications or combinations of basic forward and backward differencing. Central differencing, for example, is an implicit technique which computes the current-iteration temperatures as the arithmetic average of the forward and backward differencing predictions. As another example, exponential prediction uses the forward differencing equation but provides stability for all Δt by exponentially "derating" the $\dot{Q}_i$ terms according to the ratio of τ_i to Δt.

2.4 Modeling Parameters

The solutions to the heat transfer equation developed in the preceding sections required that continuous variables be quantized. Spatial variables were quantized through the artifices of nodes and conductors, and time was quantized into "time steps" of size Δt. By assuming, for the sake of discussion, that all nodes are cubical, with side Δx, then this Δx can be used as a general spatial quantum, and it can be related to the time quantum, Δt. For example, the forward differencing stability criterion, τ, (and therefore the maximum time step) is related to Δx as shown in equation (21):

$$\frac{\Delta x^2}{m\alpha} = \tau = \Delta t_{max} \tag{21}$$

one dimensional: $m = 2$
two dimensional: $m = 4$
three dimensional: $m = 6$

Since the finite differencing solution approaches the exact solution as Δx and Δt approach zero, it is logical to ask if anything imposes a minimum on these values. The answer is yes: cost and computer core memory space. Clearly, the latter constraint restricts Δx to an explicit non-zero minimum. That is, a small Δx means a large number of nodes and conductors, and the computer's memory must contain enough space to hold all of the parameters (capacitance, temperature, conductance, etc.) associated with these modeling elements. In addition to using much more computer time for analyses, a large model also costs more to develop than a small one.

The time step can be chosen as small as desired with a consequent increase in the computer run time required for analysis. The relationship between run time and time step size is linear for forward differencing because exactly one "iteration" is required for each time step. For implicit methods, however, the relationship is not as predictable, because

the number of iterations is controlled by the convergence criteria, N and δ. In addition, the greater the number of iterations, and the greater the number of nodes processed during each iteration, then the greater will be the susceptibility of the answers to computer round-off error.

Looking at the problem from the other direction, Δx may also be chosen large enough to include the entire thermal system in one node. The time step, however, at least for forward differencing, is limited in size to the CSGMIN. This limit is not imposed on the implicit solution techniques, although a damped oscillatory response may result when Δt is too large. Since such an oscillating response can be critically damped by using the damping factor, ζ, there is no definitive equation for the maximum Δt that may be used successfully with implicit solutions. To further complicate this understanding, there is no definitive equation for the value of ζ which will yield the most effective damping, although a value of 0.5 has been routinely used with good results.

To summarize, the thermal math-modeler is faced with the task of designing a model and selecting a solution technique which will yield good, stable answers for the least cost. To do this, the modeler must choose values for the following parameters:

Δx - node size
Δt - time step
N - iterations
δ - convergence criterion
ζ - damping factor

Forward differencing, which does not require N, δ, or ζ, and which defines at least the maximum Δt, is often chosen as the solution technique simply because it reduces the number of parameters which must be juggled about. In the hopes of leading to a more logical rationale for selecting model and solution parameters, a case study using various methods is presented in Section 3.0.

3.0 OPERATIONAL PARAMETER RELATIONSHIPS

Perhaps the interrelationship between the lumped parameter system and the particular solution techniques that are usually employed in the problem solution can be best displayed with examples:

3.1 One-Dimensional Bar of Metal

The first group of cases treats a bar of aluminum as shown in Figure 2-1.

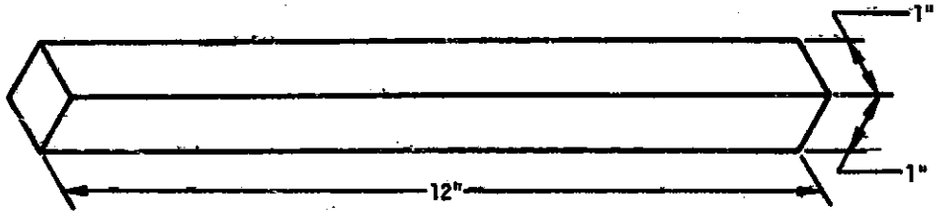

Figure 3-1. Bar of Metal

A boundary temperature of 1000°F is applied at x = 0 and a temperature of 0°F is applied at x = 12. The length of the bar radiates to deep space at -460°F. The bar is initially at 0°F and the transient response is sought at two points: x = 1 and x = 6. The following cases were run:

Case No.	Solution Method	# Nodes	Δx	Δt	N	δ	ζ
1	Forward	12	1.0	τ			
2	Forward	12	1.0	0.5τ			
3	Forward	12	1.0	0.1τ			
4	Central	12	1.0	τ	50	1.0	1.0
5	Central	12	1.0	3τ	50	1.0	1.0
6	Central	12	1.0	10τ	50	1.0	1.0
7	Backward	12	1.0	τ	50	1.0	1.0
8	Backward	12	1.0	3τ	50	1.0	1.0
9	Backward	12	1.0	10τ	50	1.0	1.0
10	Forward	3	4.0	τ			
11	Forward	6	2.0	τ			
12	Forward	24	0.5	τ			
13	Central	3	4.0	3τ	50	1.0	1.0
14	Central	6	2.0	3τ	50	1.0	1.0
15	Central	24	0.5	3τ	50	1.0	1.0
16	Backward	3	4.0	3τ	50	1.0	1.0
17	Backward	6	2.0	3τ	50	1.0	1.0
18	Backward	24	0.5	3τ	50	1.0	1.0
19	Backward	24	0.5	τ	50	1.0	1.0
20	Backward	24	0.5	τ	50	0.05	1.0

Ignoring cases 19 and 20, the bulk of the cases can be divided into two groups: (1) time step variations, and (2) node size variations. The results are shown in Figures 3-2, 3-3, 3-4, and 3-5. These figures plot accuracy vs cost in terms of temperature deviation vs node-iterations. Temperature deviation is stated in degrees F relative to a stated reference value. This value represents the apparent correct temperature which was arrived at by correlating the collection of data points produced by the various cases. The reference temperature is not (necessarily) the correct analytic answer. No attempt was made to find an analytic solution to the problem.

The product of the number of nodes times the number of iterations yields a figure that is closely related to the actual computer cost involved in

analyzing a model. For a given computer, the number of node-iterations which can be run in a given amount of time is fairly equal regardless of the solution technique. Actually, the comparison of node-iterations for a one-dimensional model versus node-iterations for a three dimensional model is not strictly reasonable since the latter model will contain more conductors per node. However, for order-of-magnitude comparisons, node-iterations represents a simple and useful measure of cost.

Figure 3-2 shows the results for x = 1 inch and t = 25 seconds. The effects of time-step variations and solution technique on a 12 node model are shown. As might be expected, it appears that the smaller the time step the greater the accuracy and the greater the cost. Since a host of minimax hypotheses could be formulated from this figure, all of which or none of which might be true, no further hypotheses will be stated here. As indicated in the Introduction, it remains for the reader to abstract from this figure as much meaningful information as he is able.

Figure 3-3 is similar to Figure 3-2, except that the effects of node size variations are emphasized. Since the Δt and δ for the implicit routines were held constant over the various cases, two additional cases are plotted for a smaller Δt and δ. Again, as might be expected, it appears that the smaller the node size, Δx, and hence, the greater the number of nodes, then the greater the accuracy and the greater the cost. Further conclusions will be left for the reader to formulate.

Figure 3-4 shows the effects of time step variations and solution technique on the results for x = 6 inches and t = 100-seconds. It will be noticed that the temperature dispersion is not as great as for x = 1 inch and t = 25 seconds. This is to be expected since the mass of the bar from x = 0 to x = 6 serves as a much more effective low pass filter, which implies greater accuracy for a given sampling frequency (i.e. Δt).

Figure 3-5 is similar to Figure 3-4 except that it highlights the effects of node size variations. For a given solution technique, it was expected that all points would lie on a smooth curve. This did not hold

for backward differencing with 24 nodes. To discover why, two additional cases were run with first, the time step, and then the time step and relaxation criterion reduced. The results indicate that the roll-off at large node-iterations was due to the accumulated relaxation error.

Figure 3-2. The Effect of a Variation in Size of Time Step for Twelve Node Model at t=25 seconds and x=1 inch

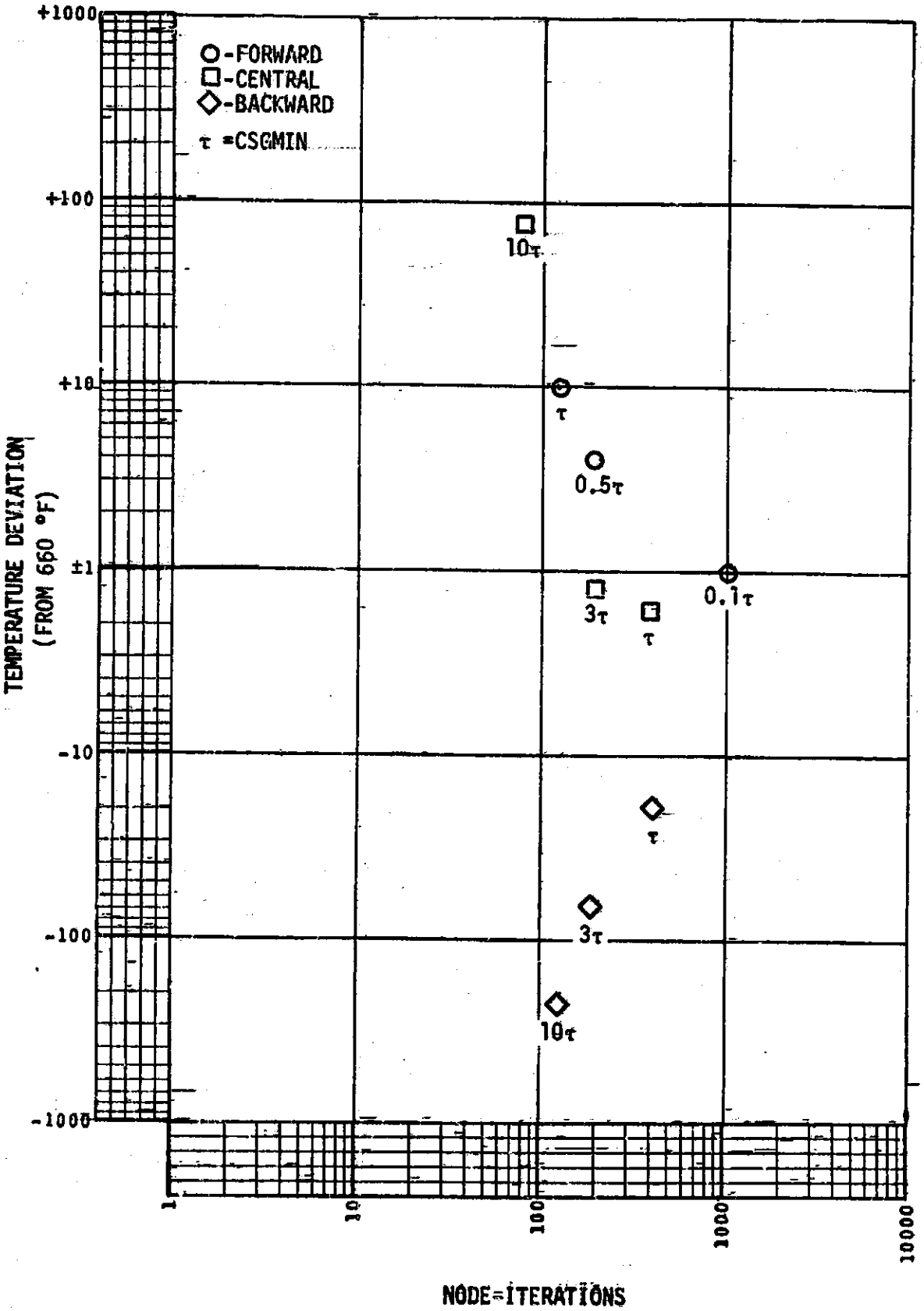

Figure 3-3. The Effect of a Variation in Node Size at t=25 seconds and x=1 inch

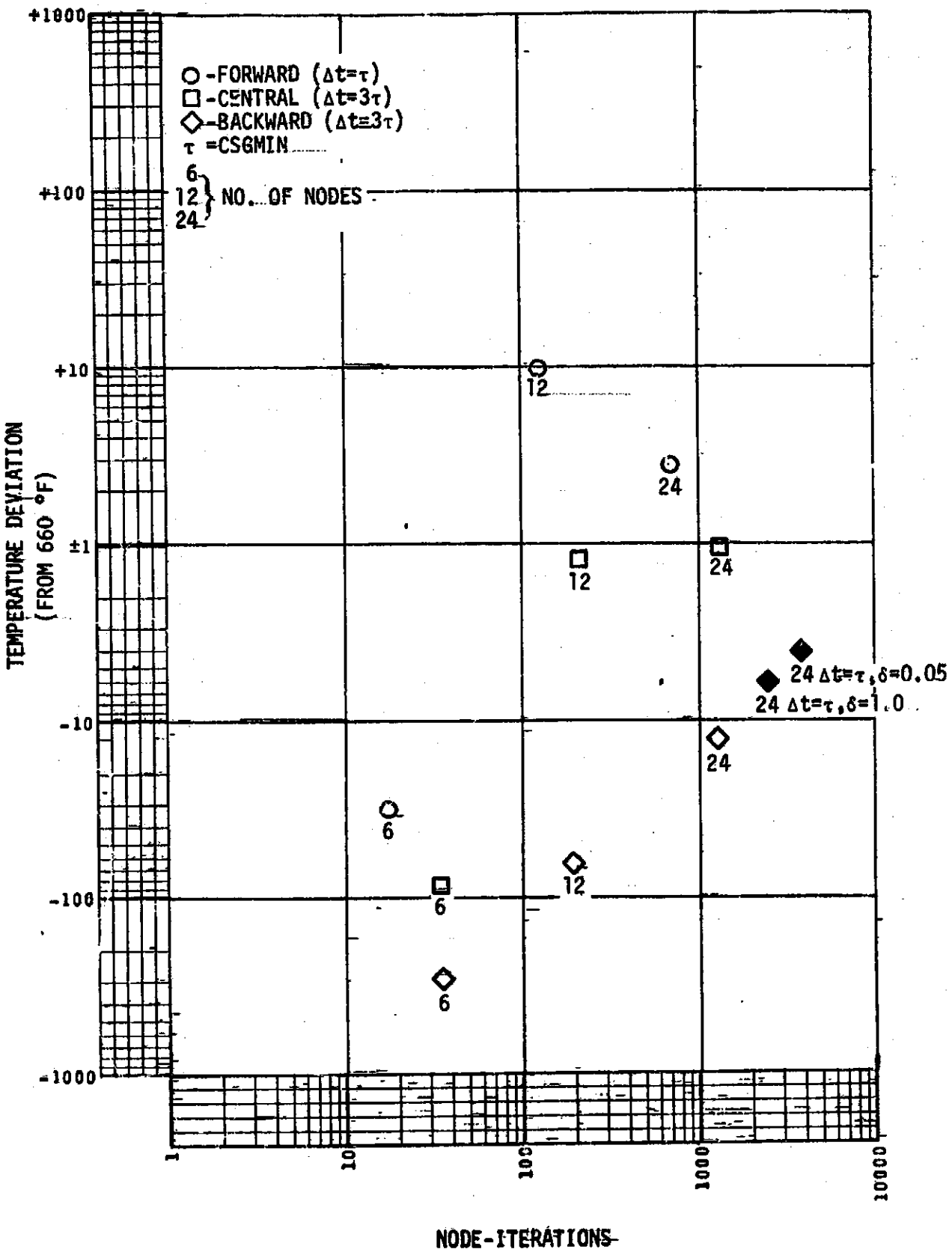

Figure 3-4. The Effect of a Variation in Size of Time Step for Twelve Node Model at t=100 seconds and x=6 inches

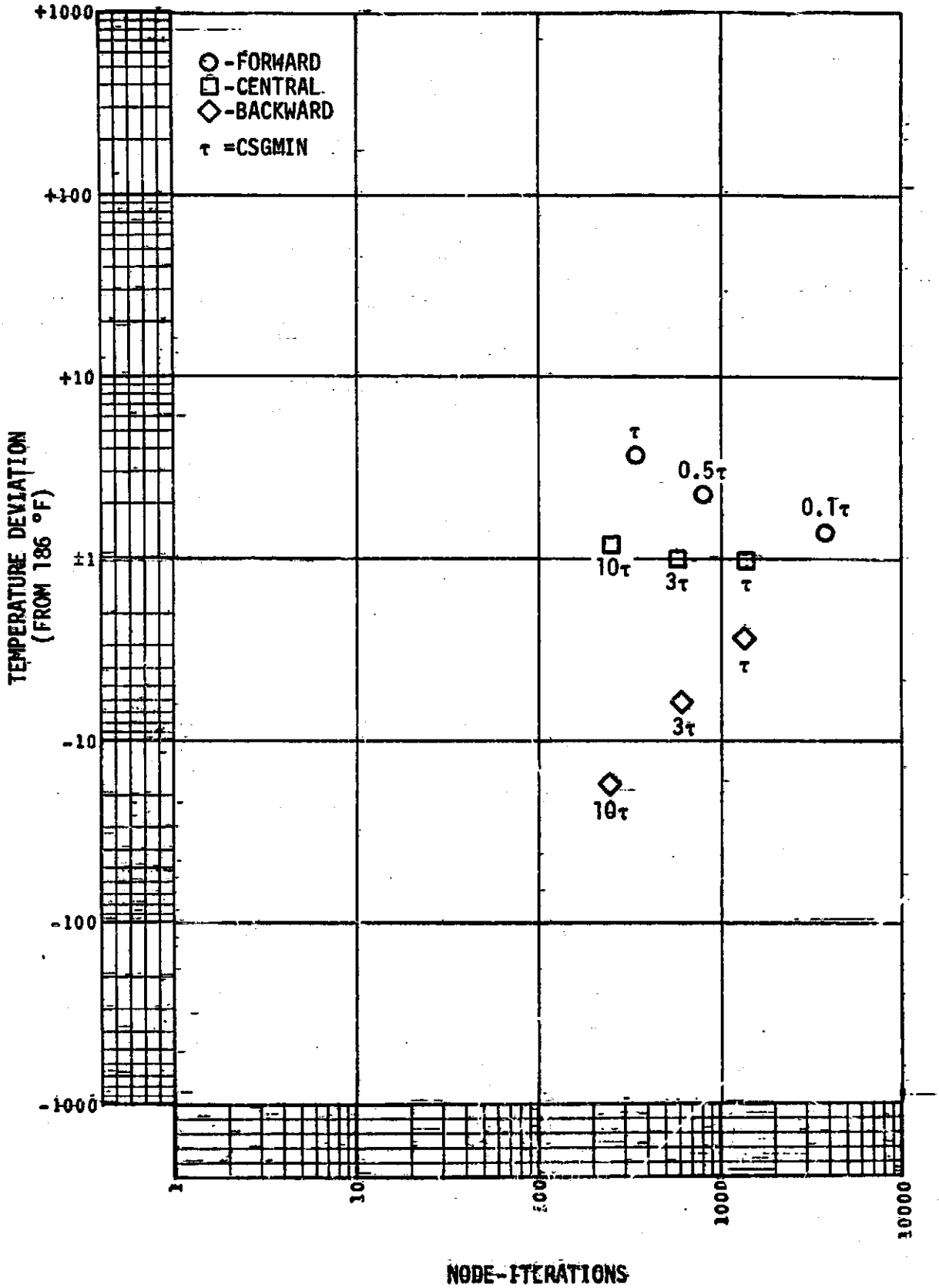

Figure 3-5. The Effect of a Variation in Node Size at t=100 seconds and x=6 inches

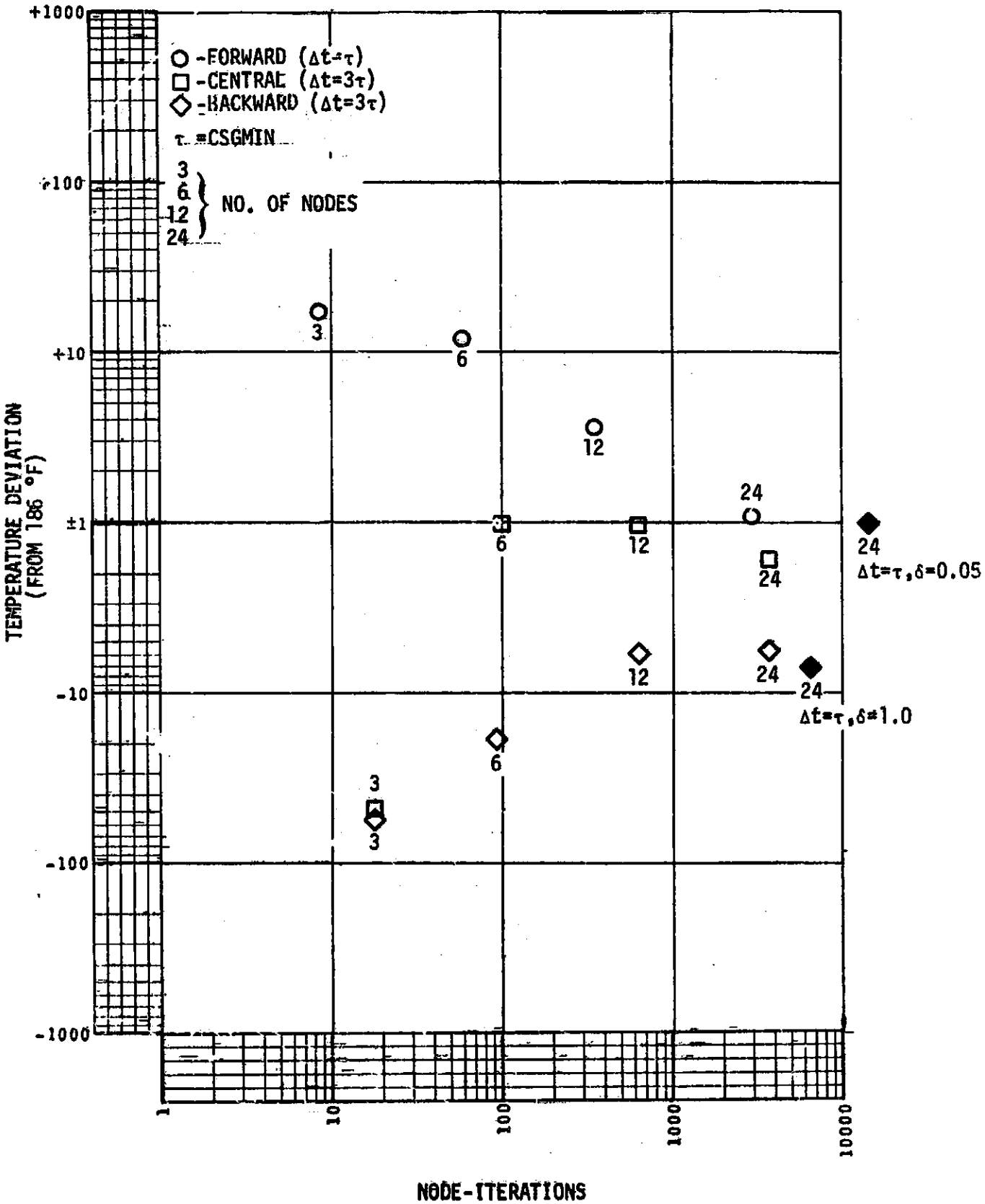

3.2 Other One-Dimensional Cases

In the discussion of Section 3.1, dimensions were retained so that the reader would have some intuitive understanding of the relative magnitudes of the various parameters. However, since the basic heat transfer equations can be cast in a dimensionless form, the results of Section 3.1 can be applied to other one-dimensional configurations, as required.

3.3 Two-Dimensional Plate of Metal

This group of cases treats a plate of aluminum, nine inches on each side and one inch thick. Boundary conditions are imposed as indicated in Figure 3-6, and the temperature at the center of the plate, 100 seconds, is desired.

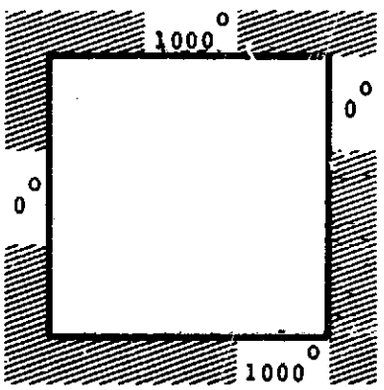

Figure 3-6. Boundary Conditions on Two-Dimensional Plate

The results of a variety of analyses of this plate are presented in Figure 3-7 and 3-8. The results in Figure 3-7 appear to be incorrectly plotted since they appear to converge to a point 10 degrees from the "assumed" answer. However, the results shown in Figure 3-8 confirm that the solution must be closer to 290°F than 280°F. The difference occurred because the model used for the cases displayed in Figure 3-7 contained only 36 nodes, and this number was evidently insufficient to accurately represent the character of the heat flow in the plate. This problem did not arise for the one-dimensional cases in Section 3.1 because the heat

flow, by definition, always followed the conductor paths exactly. In selecting finer and finer meshes for the two dimensional case, it is evident that the modelled heat flow paths (i.e., the conductors) will lie closer and closer to the actual paths, with a consequent increase in temperature prediction accuracy.

3.4 Other Two-Dimensional Cases

The principles of similarity and non-dimensional analysis may be applied to the results of Section 3.3 for other combinations of material type and dimensions.

Figure 3-7. The Effect of Variation in Time Step for Center of Plate at t=100 seconds

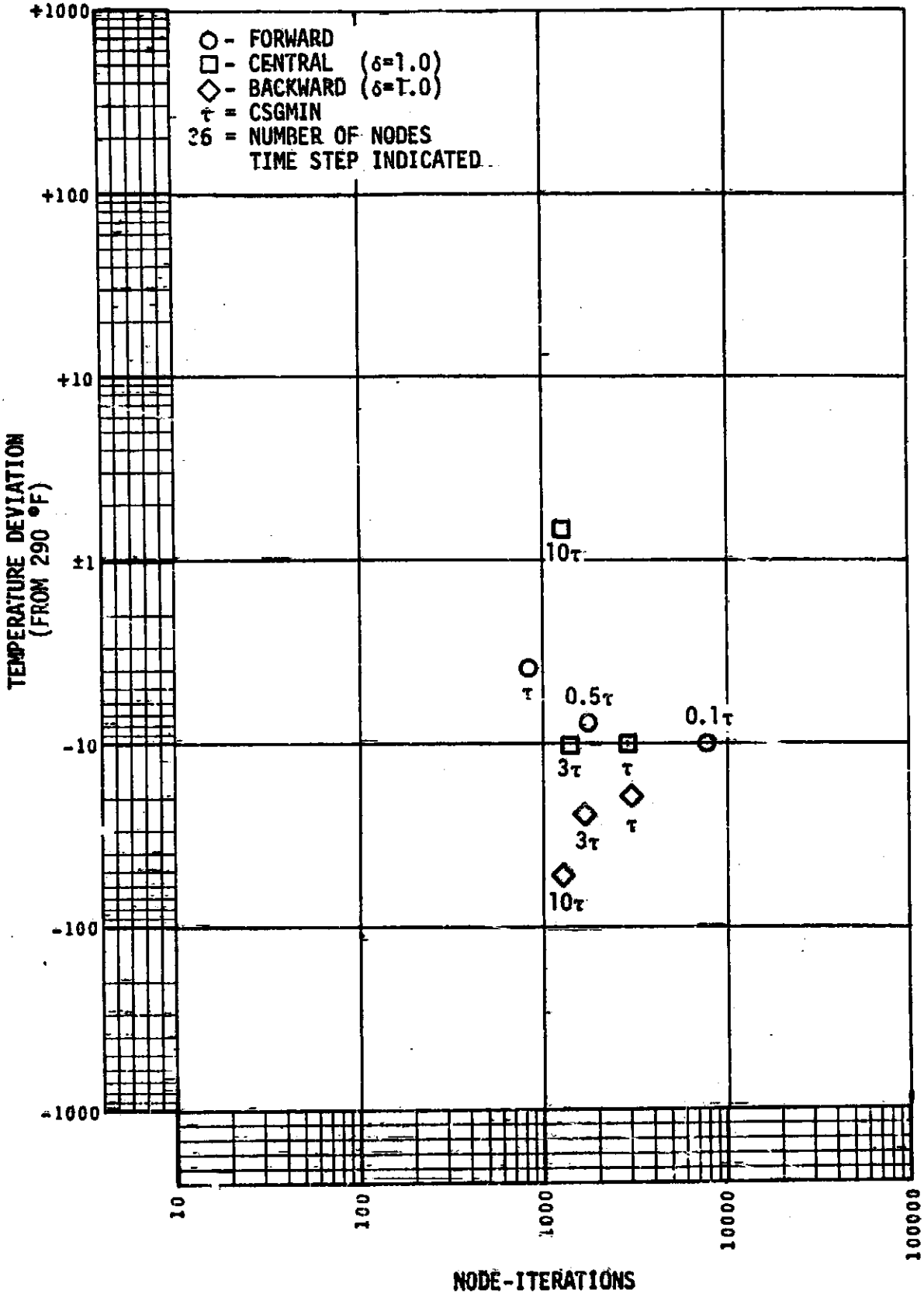

Figure 3-8. The Effect of Variation in Node Size for Center of Plate at t=100 seconds

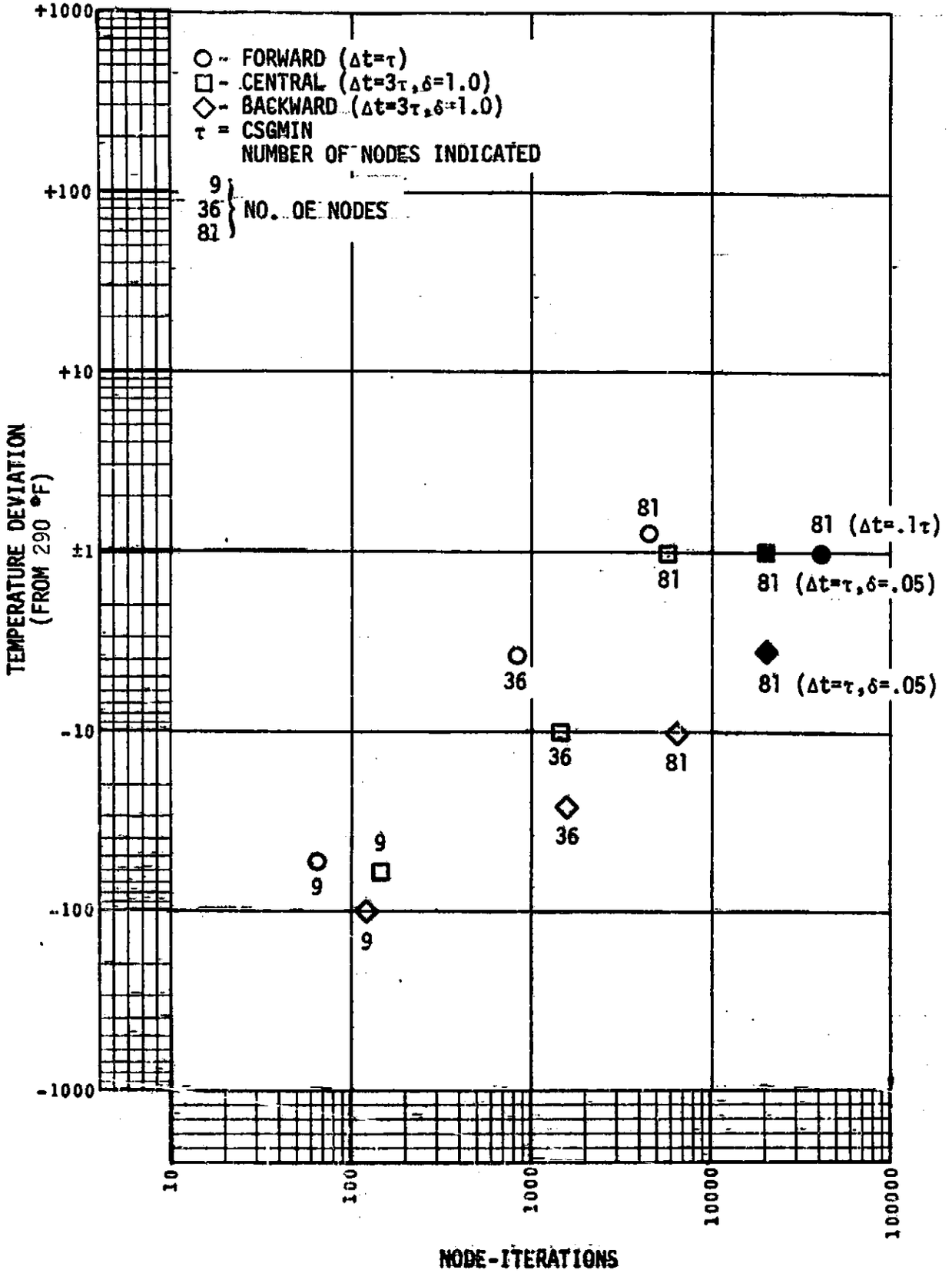

REFERENCES

1. Dusinberre, G. M., Heat Transfer Calculations by Finite Differences, International Textbook Company, 1961.

2. Kreith, F., Principles of Heat Transfer, International Textbook Company, 1965.

3. Chapman, A. J., Heat Transfer, MacMillan, 1967.

4. Elgerd, Olle I., Control Systems Theory, McGraw-Hill, 1967.

5. Ishimoto, T., SINDA Engineering Program Manual, TRW Systems, 14690-H002-R0-00, June 1971.